Research paper

Preparation of bivalent agonists for targeting the mu opioid and cannabinoid receptors

Szabolcs Dvorácskó [a], Attila Keresztes [a, 1], Adriano Mollica [b], Azzurra Stefanucci [b], Giorgia Macedonio [b], Stefano Pieretti [c], Ferenc Zádor [d], Fruzsina R. Walter [e], Mária A. Deli [e], Gabriella Kékesi [f], László Bánki [g], Gábor Tuboly [h], Gyöngyi Horváth [f], Csaba Tömböly [a, *]

[a] A Laboratory of Chemical Biology, Institute of Biochemistry, Biological Research Centre of the Hungarian Academy of Sciences, Temesvári krt. 62., 6726, Szeged, Hungary
[b] Dipartimento di Farmacia, Universita di Chieti-Pescara "G. d'Annunzio", Via dei Vestini 31, 66100, Chieti, Italy
[c] Istituto Superiore di Sanità, Centro Nazionale Ricerca e Valutazione Preclinica e Clinica dei Farmaci, Viale Regina Elena 299, 00161, Rome, Italy
[d] Laboratory of Opioid Research, Institute of Biochemistry, Biological Research Centre of the Hungarian Academy of Sciences, Temesvári krt. 62., 6726, Szeged, Hungary
[e] Biological Barriers Research Group, Institute of Biophysics, Biological Research Centre of the Hungarian Academy of Sciences, Temesvári krt. 62., 6726, Szeged, Hungary
[f] Department of Physiology, Faculty of Medicine, University of Szeged, 6720, Szeged, Dóm tér 10., Hungary
[g] Department of Traumatology, Faculty of Medicine, University of Szeged, 6725, Szeged, Semmelweis u. 6., Hungary
[h] Department of Neurology, Faculty of Medicine, University of Szeged, 6725, Szeged, Semmelweis u. 6., Hungary

ARTICLE INFO

ABSTRACT

In order to obtain novel pharmacological tools and to investigate a multitargeting analgesic strategy, the CB_1 and CB_2 cannabinoid receptor agonist JWH-018 was conjugated with the opiate analgesic oxycodone or with an enkephalin related tetrapeptide. The opioid and cannabinoid pharmacophores were coupled via spacers of different length and chemical structure. In vitro radioligand binding experiments confirmed that the resulting bivalent compounds bound both to the opioid and to the cannabinoid receptors with moderate to high affinity. The highest affinity bivalent derivatives **11** and **19** exhibited agonist properties in [^{35}S]GTPγS binding assays. These compounds activated MOR and CB (**11** mainly CB_2, whereas **19** mainly CB_1) receptor-mediated signaling, as it was revealed by experiments using receptor specific antagonists. In rats both **11** and **19** exhibited antiallodynic effect similar to the parent drugs in 20 μg dose at spinal level. These results support the strategy of multitargeting G-protein coupled receptors to develop lead compounds with antinociceptive properties.

© 2019 Elsevier Masson SAS. All rights reserved.

1. Introduction

Mu opioid receptor (MOR) agonists are the most common therapeutics in clinic to alleviate severe pain. However, their dose-limiting adverse effects inspire the development of novel analgesics [1]. Cannabinoid (CB) receptor agonists can modulate hyperalgesia and show effective therapeutic value against inflammatory and chronic pain including neuropathic pain [2]. The co-administration of MOR and CB receptor agonists has been shown to enhance the antinociceptive effect with decreased opiate-related side-effects, and the synergism of opioid and cannabinoid ligands has been extensively studied [3] in mice [4—11], in rats [12—15], in rhesus monkeys [16—19] and in an experimental pain model applied to volunteers [20].

Initiated by the possible dimerization interaction of the opioid and cannabinoid receptors [21—23] bivalent compounds, i.e. spacer linked pharmacophores, were also considered to decrease the opioid side-effects. Conjugating the MOR agonist fentanyl to the CB_1 antagonist/inverse agonist rimonabant resulted in MOR-CB

antagonists [24]. Coupling of an enkephalin-related peptide to rimonabant led to the loss of analgesic effects in hot plate and tail flick tests [25]. In contrast, bivalent compounds of the MOR agonist α-oxymorphamine and a rimonabant analogue with oxydiacetic acid-based spacers were found to exhibit antinociception in tail flick test without producing tolerance in 24 h [26]. Another important goal of the combination treatments is to decrease the effective dose of opioids, especially in the treatment of severe chronic pains. It could be potentially achieved by combining opioid agonists with cannabinoid agonists [3,27—30]. In a case study of a patient with familial Mediterranean fever it was reported that the administration of Δ^9-tetrahydrocannabinol (Δ^9-THC) reduced the morphine consumption by about 50% to alleviate chronic pain [27].

In order to target the MOR and CB receptors with a single compound, bivalent ligands consisting of a MOR and a CB agonist were designed. In one set the MOR agonist oxycodone [1,31—33], that is widely used in the treatment of severe pain [34] was applied. The other set contained the enkephalin-related tetrapeptide Tyr-d-Ala-Gly-Phe [35—37] as the opioid pharmacophore. Both opioid agonists were coupled with naphthalen-1-yl(1-pentyl-1*H*-indol-3-yl)methanone (JWH-018 or AM 678), a full CB agonist. JWH-018 is an indole-type synthetic CB receptor agonist that structurally relates to WIN-55,212—2. It exhibits typical cannabinoid pharmacology in vivo and has high affinity for both CB receptors ($K_i(CB_1) = 9.00$ nM, $K_i(CB_2) = 2.94$ nM) [38—41]. The receptor binding and signaling properties of the resulting bivalent compounds were investigated and the in vitro active compounds were tested in vivo after spinal administration for antinociception in a chronic pain model, which might be clinically relevant.

2. Materials and methods

2.1. General

The purity of all reagents and solvents were analytical or the highest commercially available grade. Starting materials, buffer components, GDP, GTPγS were purchased from Sigma-Aldrich Kft. (Budapest, Hungary), fatty acid free bovine serum albumin (BSA) was from Serva (Heidelberg, Germany), DAMGO was obtained from Bachem AG (Bubendorf, Switzerland), Ile^{5,6}-deltorphin-2 was prepared in the Laboratory of Chemical Biology (BRC, Hungary), naloxone was kindly provided by Endo Laboratories (Wilmington, DE, USA), WIN-55,212—2 was purchased from Tocris Inc. (Bristol, UK), [^{35}S]GTPγS (s.a. >37 TBq/mmol) was purchased from Hartmann Analytic (Braunschweig, Germany). The radioligands [^{3}H]JWH-018 (s.a. 1.48 TBq/mmol), [^{3}H]WIN-55,212—2 (s.a. 485 GBq/mmol), [^{3}H]DAMGO (s.a. 1.43 TBq/mmol), [^{3}H]Ile^{5,6}-deltorphin-2 (s.a. 725 GBq/mmol) and [^{3}H]HS-665 (s.a. 1.13 TBq/mmol) were prepared in the Laboratory of Chemical Biology (BRC, Hungary). Tritium labeling was carried out in a self-designed vacuum manifold [42] and radioactivity was measured with a Packard Tri-Carb 2100 TR liquid scintillation analyser using Insta Gel scintillation cocktail of PerkinElmer. Analytical thin layer chromatography (TLC) was performed on 5×10 cm glass plates precoated with silica gel 60 F$_{254}$ (Merck, Darmstadt, Germany), spots were visualized with UV light. Flash chromatography was carried out on silica gel 60 (Sigma Ltd., St. Louis, MO, USA) using the indicated solvents. Analytical HPLC separations were performed with a Merck-Hitachi LaChrom system on an Alltech Altima HP C18 (150×4.6 mm, $5\,\mu$m) or on a Vydac 218TP54 (250×4.6 mm, $5\,\mu$m) column using the indicated gradients of ACN (0.08% (v/v) TFA) (eluent B) in H$_2$O (0.1%(v/v) TFA) (eluent A) at a flow rate of 1 mL/min, and UV detection at $\lambda = 216$ nm was applied. Radio-HPLC was performed on a Phenomenex Luna C18(2) (150×4.6 mm, $5\,\mu$m) column using a Jasco HPLC system equipped with a Packard Radiomatic 505 TR Flow Scintillation Analyser. ^{1}H and ^{13}C NMR spectra were recorded on a Bruker Avance 500 MHz or on a Varian Mercury 300 MHz spectrometer and chemical shifts (δ) are reported in ppm after calibration to the solvent signals. The assignments are based on ^{1}H, ^{13}C(DEPT), HSQC, HMBC, GQ-COSY and 2D-TOCSY experiments, and on the reported assignment of JWH-018 [43]. Molecular weight of the compounds was determined by ESI-MS analysis on a Finnigan

Mat LCQ spectrometer.

2.2. Oxycodone O-carboxymethyloxime (1)

Oxycodone (1 g, 3.17 mmol) was dissolved in 250 mL of EtOH then 365 mg of 2-(aminooxy)acetic acid hemihydrochloride (3.32 mmol) and 400 μL of pyridine were added. The solution was stirred at 80 °C for 75 min then the precipitate was filtered and dried under vacuum. The crude product was purified by HPLC on a Vydac 218TP1010 column (250 × 10 mm, 10 μm) using a linear gradient of 10 → 50% B in A over 25 min at a flow rate of 4 mL/min ($\lambda = 216$ nm) to give 1.14 g (93%) of pure 1 as a white solid. R_f 0.26 (CHCl$_3$−MeOH−NH$_{3(aq)}$ 9:1:0.1); HPLC k' = 4.90 (t_R = 12.4 min, linear gradient of 5 → 30% B in A over 25 min, flow rate: 1 mL/min, $\lambda = 216$ nm); ^{1}H NMR (500 MHz, MeOD) δ 6.88 (d, 1H, $J = 8.2$ Hz, 2-H), 6.79 (d, 1H, $J = 8.2$ Hz, 1-H), 5.03 (s, 1H, 5-H), 4.54 and 4.53 (2 × s, 2 × 1H, CH$_2$-COOH), 3.85 (s, 3H, OCH$_3$), 3.59 (d, 1H, $J = 6.4$ Hz, 9-H), 3.47 (d, 1H, $J = 19.9$ Hz, 10-H), 3.19 (dd, 1H, $J = 13.0, 4.6$ Hz, 16-H), 3.11 (dd, 1H, $J = 19.9, 6.4$ Hz, 10-H'), 2.93 (s, 3H, NCH$_3$), 2.87 (dd, 1H, $J = 13.0, 3.9$ Hz, 16-H'), 2.72 (ddd, 1H, $J = 17.3, 7.0, 2.2$ Hz, 15-H), 2.62 (m, 2H, 7-H, 15-H'), 1.75 (m, 1H, 7-H'), 1.71 (dd, 1H, $J = 7.0, 2.6$ Hz, 8-H), 1.46 (ddd, 1H, $J = 14.1, 11.5, 7.0$ Hz, 8-H'); ^{13}C NMR (126 MHz, MeOD) δ 175.6 (COOH), 156.7 (C-6), 146.7 (C-4), 144.8 (C-3), 130.1 (C-12), 124.2 (C-11), 121.1 (C-1), 117.7 (C-2), 87.5 (C-5), 72.9 (O-CH$_2$-COOH), 71.2 (C-14), 68.3 (C-9), 57.7 (OCH$_3$), 48.3 (C-16), 47.2 (C-13), 41.7 (NCH$_3$), 30.0 (C-7), 28.9 (C-8), 24.7 (C-10), 18.6 (C-15); ESI-MS calcd for C$_{20}$H$_{24}$N$_2$O$_6$ 388.16, found 388.59 [M+H]$^+$.

2.3. Oxycodone O-(N-(2-(N-Boc-amino)ethyl)carboxamidomethyl) oxime (2)

Oxime 1 (20 mg, 51.5 μmol) and HOBt.H$_2$O (7.9 mg, 51.5 μmol) were dissolved in 1.5 mL of DMF and DIC (8 μL, 51.5 μmol) was added. It was stirred for 5 min, then tert-butyl 2-aminoethylcarbamate hydrochloride (20 mg, 102 μmol) and DIEA (18 μL, 102 μmol) were added to the solution. The mixture was stirred at 50 °C for 16 h then it was evaporated in vacuo. The crude product was purified by column chromatography on silica gel 60 with CHCl$_3$−MeOH (8:2) to give 22.2 mg (81%) of 2 as yellowish oil. R_f 0.45 (CHCl$_3$−MeOH 9:1); HPLC k' = 4.65 (t_R = 11.9 min, linear gradient of 10 → 60% B in A over 25 min); ^{1}H NMR (500 MHz, CDCl$_3$) δ 6.83 (brs, 1H, 2-H), 6.74 (d, 1H, $J = 8.2$ Hz, 1-H), 6.58 (brs, CONH), 5.88 (brs, 1H, CONH), 5.07 and 5.01 (2 × s, 1H, 5-H), [4.68 and 4.58 (2 × d, $J = 16.9$ Hz), 4.53 (d, $J = 16.0$ Hz)] (2H, O-CH$_2$-CO), 3.90 (s, 3H, OCH$_3$), 3.71 (m, 1H, 9-H), 3.28 (overlapping m, 6H, 1''-H, 2''-H, 10-H, 16-H), 3.08 (d, 1H, $J = 18.5$ Hz, 10-H'), 2.90 (brs, 4H, NCH$_3$, 15-H), 2.77 (m, 2H, 7-H, 16-H'), 2.33 (m, 1H, 15-H'), 1.80 (m, 2H, 7-H', 8-H), 1.48 (m, 1H, 8-H'), 1.40 (s, 9H, C(CH$_3$)$_3$); ESI-MS calcd for C$_{27}$H$_{38}$N$_4$O$_7$ 530.27, found 531.30 [M+H]$^+$.

2.4. Oxycodone O-(N-(6-(N-Boc-amino)hexyl)carboxamidomethyl) oxime (3)

Prepared as described for 2 but tert-butyl 6-aminohexylcarbamate (22 mg, 102 μmol) was used. The crude product was purified by column chromatography on silica gel 60 with CHCl$_3$−MeOH (8:2) to give 23.1 mg (77%) of 3 as pale yellow oil. R_f 0.44 (CHCl$_3$−MeOH 9:1); HPLC k' = 6.76 (t_R = 16.3 min, linear gradient of 10 → 60% B in A over 25 min); ^{1}H NMR (500 MHz, CDCl$_3$) δ 6.83 (d, 1H, $J = 8.2$ Hz, 2-H), 6.74 (d, 1H, $J = 8.2$ Hz, 1-H), 6.09 (t, 1H, $J = 5.1$ Hz, CONH), 5.05 (s, 1H, 5-H), [4.60 and 4.52 (2 × d, 2 × 1H, $J = 15.7$ Hz, O-CH$_2$-CO), 3.90 (s, 3H, OCH$_3$), 3.85 (m, 1H, 9-H), 3.27 (overlapping m, 4H, 1''-H, 6''-H), 3.08 (m, 3H, 10-H, 10-H', 16-H), 2.91 (s, 3H, NCH$_3$), 2.82 (m, 2H, 7-H, 16-H'), 2.71 (brs, 1H, 15-H), 2.33 (m, 1H, 15-H'), 1.85 (brs, 1H, 8-H), 1.77 (d, 1H, $J = 9.7$ Hz,

7-H'), 1.47 (m, 5H, 2''-H, 5''-H, 8-H'), 1.43 (s, 9H, C(CH$_3$)$_3$), 1.31 (m, 4H, 3''-H, 4''-H); ESI-MS calcd for C$_{31}$H$_{46}$N$_4$O$_7$ 586.34, found 587.40 [M+H]$^+$.

2.5. Oxycodone O-(N-(13-(N-Boc-amino)-4,7,10-trioxatridecyl) carboxamidomethyl)oxime (4)

Prepared as described for 2 but N-Boc-4,7,10-trioxa-1,13-tridecanediamine (33 mg, 102 μmol) was used. The crude product was purified by column chromatography on silica gel 60 with CHCl$_3$−MeOH (8:2) to give 23.6 mg (66%) of 4 as yellowish oil. R_f 0.52 (CHCl$_3$−MeOH 9:1); HPLC k' = 4.94 (t_R = 12.5 min, linear gradient of 5 → 95% B in A over 25 min); ^{1}H NMR (500 MHz, CDCl$_3$) δ 6.82 (d, 1H, $J = 8.2$ Hz, 2-H), 6.73 (d, 1H, $J = 8.2$ Hz, 1-H), 6.43 (brs, CONH), 5.06 (s, 1H, 5-H), 5.01 (brs, CONH), 4.58 and 4.51 (2 × d, 2 × 1H, $J = 15.8$ Hz, O-CH$_2$-CO), 3.90 (s, 3H, OCH$_3$), 3.84 (m, 1H, 9-H), (3.61, 3.57, 3.52) (3 × m, 12H, 3''-H, 5''-H, 6''-H, 8''-H, 9''-H, 11''-H), 3.43−3.19 (overlapping m, 6H, 1''-H, 13''-H, 10-H, 16-H), 3.08 (dd, 1H, $J = 19.6, 6.0$ Hz, 10-H') 2.90 (s, 3H, NCH$_3$), 2.81 (m, 3H, 7-H, 15-H, 16-H'), 2.69 (m, 1H, 15-H'), 1.83 (m, 1H, 8-H), 1.74 (m, 5H, 7-H', 2''-H, 12''-H), 1.44 (m, 1H, 8-H'), 1.43 (s, 9H, C(CH$_3$)$_3$); ESI-MS calcd for C$_{35}$H$_{54}$N$_4$O$_{10}$ 690.38, found 691.15 [M+H]$^+$.

2.6. Oxycodone O-(N-(2-aminoethyl)carboxamidomethyl)oxime (5)

The N-protected oxime 2 (22 mg, 41.5 μmol) was dissolved in 2 mL of DCM containing 50% (v/v) TFA and it was stirred for 30 min at rt. The solution was evaporated in vacuo that yielded the TFA salt of 5. 21 mg (95%); R_f 0.27 (CHCl$_3$−MeOH 9:1); HPLC k' = 3.64 (t_R = 10.2 min, linear gradient of 5 → 30% B in A over 25 min); ESI-MS calcd for C$_{22}$H$_{30}$N$_4$O$_5$ 430.22, found 431.30 [M+H]$^+$.

2.7. Oxycodone O-(N-(6-aminohexyl)carboxamidomethyl)oxime (6)

Prepared as described for 5. Yield 22 mg (96%); R_f 0.26 (CHCl$_3$−MeOH 9:1); HPLC k' = 4.90 (t_R = 12.4 min, linear gradient of 5 → 95% B in A over 25 min); ESI-MS calcd for C$_{26}$H$_{38}$N$_4$O$_5$ 486.28, found 487.11 [M+H]$^+$.

2.8. Oxycodone O-(N-(13-amino-4,7,10-trioxatridecyl) carboxamidomethyl)oxime (7)

Prepared as described for 5. Yield 22.5 mg (95%); R_f 0.33 (CHCl$_3$−MeOH 9:1); HPLC k' = 4.82 (t_R = 12.8 min, linear gradient of 5 → 30% B in A over 25 min); ESI-MS calcd for C$_{30}$H$_{46}$N$_4$O$_8$ 590.33, found 591.09 [M+H]$^+$.

2.9. 6-(1H-indol-1-yl)hexanoic acid (8)

To a stirred solution of indole (1.17 g, 10 mmol) in ACN (10 mL) were added triethylamine (1.39 mL, 10 mmol) and 6-bromohexanoic acid (1.94 g, 10 mmol), then the solution was stirred at 80 °C for 16 h. The solvent was evaporated in vacuo and the residue was extracted with water and CHCl$_3$ (3 × 20 mL). The combined organic phase was washed with brine, and dried over Na$_2$SO$_4$. After evaporation the crude product was purified by column chromatography on silica gel 60 with EtOAc−n-hexane 2:1 to give 1.76 g (77%) of pure 8 as yellow oil. R_f 0.38 (EtOAc−n-hexane 2:1); HPLC k' = 4.36 (t_R = 15.0 min, linear gradient of 5 → 60% B in A over 25 min); ^{1}H NMR (500 MHz, CDCl$_3$) δ 7.63 (d, 1H, $J = 7.9$ Hz, 4-H), 7.33 (d, 1H, $J = 8.2$ Hz, 7-H), 7.20 (t, 1H, $J = 7.6$ Hz, 5-H), 7.10 (t, 1H, $J = 7.6$ Hz, 6-H), 7.09 (d, 1H, $J = 3.2$ Hz, 2-H), 6.48 (d, 1H, $J = 3.1$ Hz, 3-H), 4.13 (t, 2H, $J = 7.1$ Hz, 1'-H), 2.33 (t, 2H, $J = 7.4$ Hz, 5'-

H), 1.87 (quin, 2H, $J = 7.3$ Hz, 2′-H), 1.67 (quin, 2H, $J = 7.5$ Hz, 4′-H), 1.38 (quin, 2H, $J = 7.7$ Hz, 3′-H); ^{13}C NMR (126 MHz, CDCl$_3$) δ 178.2 (COOH), 136.0 (C-7a), 128.7 (C-3a), 127.9 (C-2), 121.5 (C-6), 121.1 (C-4), 119.4 (C-5), 109.4 (C-7), 101.1 (C-3), 46.3 (C-1′), 33.8 (C-5′), 30.1 (C-2′), 26.6 (C-3′), 24.4 (C-4′); ESI-MS calcd for C$_{14}$H$_{17}$NO$_2$ 231.13, found 231.93 [M+H]$^+$.

2.10. 6-(3-(1-Naphthoyl)-1H-indol-1-yl)hexanoic acid (9)

To a stirred solution of **8** (1.5 g, 6.49 mmol) in 5 mL of dry DCM 6.5 mL of 1 M Et$_2$AlCl in hexane (6.49 mmol) was added dropwise. It was stirred at 0 °C for 1 h then 1.2 g of 1-naphthoyl chloride (6.49 mmol) dissolved in 3 mL of DCM was added dropwise. The reaction mixture was stirred at 0 °C for 16 h then it was carefully poured into a mixture of ice and 0.1 M HCl and it was extracted with DCM. The combined organic phase was washed with brine and dried over Na$_2$SO$_4$. The organic phase was evaporated and the crude product was purified by column chromatography on silica gel 60 with (EtOAc−n-hexane 1:1) to give 1.05 g (42%) of pure **9** as yellow oil that became crystalline in a day. R$_f$ 0.26 (EtOAc−n-hexane 2:1); HPLC k' = 5.07 (t$_R$ = 17.0 min, linear gradient of 20 → 100% B in A over 25 min); ^{1}H NMR (500 MHz, CDCl$_3$) δ 8.50 (m, 1H, 4-H), 8.19 (d, 1H, $J = 8.3$ Hz, 15′-H), 7.98 (d, 1H, $J = 8.2$ Hz, 11′-H), 7.92 (d, 1H, $J = 8.1$ Hz, 12′-H), 7.67 (d, 1H, $J = 7.0$ Hz, 9′-H), [7.54 (t, 1H, $J = 8.2$ Hz) and 7.52 (t, 1H, $J = 8.2$ Hz)] (10′-H and 13′-H), 7.47 (t, 1H, $J = 7.1$ Hz, 14′-H), 7.41−7.34 (overlapping m, 4H, 2-H, 5-H, 6-H, 7-H), 4.08 (t, 2H, $J = 7.3$ Hz, 1′-H), 2.26 (t, 2H, $J = 7.4$ Hz, 5′-H), 1.83 (quin, 2H, $J = 7.4$ Hz, 2′-H), 1.62 (quin, 2H, $J = 7.6$ Hz, 4′-H), 1.31 (m, 2H, 3′-H); ^{13}C NMR (126 MHz, CDCl$_3$) δ 192.5 (3-CO), 181.6 (COOH), 138.9 (C-8′), 137.6 (C-2), 136.9 (C-7a), 133.8 (C-11a′), 130.6 (C-15a′), 130.4 (C-11′), 128.4 (C-12′), 127.0 (C-14′), 126.8 (C-3a), 126.5 (C-13′), 126.0 (C-9′), 125.7 (C-15′), 124.7 (C-10′), 123.3 (C-6), 122.7 (C-5), 122.2 (C-4), 117.4 (C-3), 110.1 (C-7), 46.4 (C-1′), 37.3 (C-5′), 29.9 (C-2′), 26.3 (C-3′), 25.3 (C-4′); ESI-MS calcd for C$_{25}$H$_{23}$NO$_3$ 385.17, found 386.03 [M+H]$^+$.

2.11. Bivalent compound 10

The carboxylic acid **9** (7.4 mg, 19 μmol) and HOBt.H$_2$O (2.9 mg, 19 μmol) were dissolved in 1.5 mL of DMF and DIC (2.9 μL, 19 μmol) was added. It was stirred for 5 min, then **5** (20.7 mg, 38 μmol) and DIEA (6.6 μL, 38 μmol) were added and the solution was stirred at 50 °C for 16 h. Then it was evaporated in vacuo and the crude product was purified by semipreparative HPLC on a Vydac 218TP1010 column that yielded 12.1 mg of **10** (79%) as yellow oil. R$_f$ 0.63 (CHCl$_3$−MeOH 9:1); HPLC k' = 5.82 (t$_R$ = 14.3 min, linear gradient of 10 → 100% B in A over 25 min); ^{1}H NMR (500 MHz, CDCl$_3$) δ ^{1}H NMR (CDCl$_3$) δ 8.40 (d, 1H, $J = 6.8$ Hz, 4′-H), 8.15 (d, 1H, $J = 8.4$ Hz, 15′-H), 7.96 (d, 1H, $J = 8.1$ Hz, 11′-H), 7.90 (d, 1H, $J = 8.1$ Hz, 12′-H), 7.65 (d, 1H, $J = 6.8$ Hz, 9′-H), 7.52 (t, 1H, $J = 7.6$ Hz, 10′-H), 7.50 (t, 1H, $J = 7.5$ Hz, 13′-H), 7.45 (t, 1H, $J = 7.6$ Hz, 14′-H), 7.41 (s, 1H, 2′-H), 7.39 (s, 1H, 7′-H), 7.32 (m, 2H, 5′-H, 6′-H), 6.81 (d, 1H, $J = 8.2$ Hz, 2-H), 6.74 (brs, CONH), 6.72 (d, 1H, $J = 8.2$ Hz, 1-H), 6.43 (brs, CONH), 4.99 (s, 1H, 5-H), 4.57 and 4.47 (2 × d, 2 × 1H, $J = 16.1$ Hz, O-CH$_2$-CO), 4.08 (t, 2H, $J = 6.9$ Hz, 16′-H), 3.85 (s, 3H, OCH$_3$), 3.73 (brs, 1H, 9-H), 3.26 (2 × brs, 5H, 1″-H, 2″-H, 16-H), 3.21 (d, 1H, $J = 19.0$ Hz, 10-H), 3.00 (d, 1H, $J = 19.0$ Hz, 10-H′), 2.84 (s, 4H, NCH$_3$, 15-H), 2.73 (brs, 2H, 7-H, 16-H′), 2.40 (d, 1H, $J = 8.2$ Hz, 15-H′), 2.09 (t, 2H, $J = 5.7$ Hz, 20′-H), 1.81 (quin, 2H, $J = 7.1$ Hz, 17′-H), 1.76 (m, 1H, 8-H), 1.65 (d, 1H, $J = 8.0$ Hz, 7-H′), 1.56 (quin, 2H, 6.9 Hz, 19′-H), 1.35 (m, 1H, 8-H′), 1.27 (m, 2H, 18′-H); ^{13}C NMR (126 MHz, CDCl$_3$) δ 192.3 (Ar-CO), 174.3 (20′-CONH), 170.9 (O-CH$_2$-$\underline{C}$ONH), 156.7 (C-6), 145.9 (C-4), 143.8 (C-3), 139.0 (C-8′), 138.2 (C-2′), 137.2 (C-7a′), 133.9 (C-11a′), 130.9 (C-15a′), 130.2 (C-11′), 128.6 (C-12), 128.4 (C-12′), 127.1 (C-3a′), 126.9 (C-14′), 126.5 (C-13′), 126.1 (C-9′), 126.0 (C-15′),

124.8 (C-10′), 123.8 (C-6′), 123.0 (C-5′), 122.9 (C-4′), 121.6 (C-11), 120.0 (C-1), 117.6 (C-3′), 115.8 (C-2), 110.3 (C-7′), 86.9 (C-5), 73.2 (O-$\underline{C}$H$_2$-CO), 70.4 (C-14), 65.7 (C-9), 56.8 (OCH$_3$), 47.3 (C-16), 47.1 (C-16′), 46.2 (C-13), 42.1 (NCH$_3$), 39.8 and 39.6 (C-1″, C-2″), 36.1 (C-20′), 29.6 (C-17′), 29.3 (C-7), 28.6 (C-8), 26.4 (C-18′), 25.1 (C-19′), 24.1 (C-10), 17.3 (C-15); MALDI-MS calcd for C$_{47}$H$_{51}$N$_5$O$_7$ 797.38, found 798.34 [M+H]$^+$.

2.12. Bivalent compound 11

Prepared as described for **10**, but **6** (23 mg, 38 μmol) was used. Yield 11.6 mg of **11** (71%) as brown oil. R$_f$ 0.60 (CHCl$_3$−MeOH 9:1); HPLC k' = 6.18 (t$_R$ = 15.1 min, linear gradient of 10 → 100% B in A over 25 min); ^{1}H NMR (500 MHz, CDCl$_3$) δ 8.41 (d, 1H, $J = 7.5$ Hz, 4′-H), 8.14 (d, 1H, $J = 8.3$ Hz, 15′-H), 7.96 (d, 1H, $J = 8.2$ Hz, 11′-H), 7.90 (d, 1H, $J = 8.1$ Hz, 12′-H), 7.63 (d, 1H, $J = 6.6$ Hz, 9′-H), 7.52 (t, 1H, $J = 7.9$ Hz, 10′-H), 7.50 (t, 1H, $J = 8.2$ Hz, 13′-H), 7.44 (t, 1H, $J = 7.6$ Hz, 14′-H), 7.38 (overlapping d, 1H, 7′-H), 7.37 (s, 1H, 2′-H), 7.33 (m, 2H, 5′-H, 6′-H), 6.81 (d, 1H, $J = 8.2$ Hz, 2-H), 6.72 (d, 1H, $J = 8.3$ Hz, 1-H), 6.26 (brs, 1H, 1″-NH), 6.06 (brs, 6″-NH), 5.00 (s, 1H, 5-H), 4.58 and 4.50 (2 × d, 2 × 1H, $J = 15.9$ Hz, O-CH$_2$-CO), 4.07 (t, 2H, $J = 6.8$ Hz, 16′-H), 3.85 (s, 3H, OCH$_3$), 3.78 (brs, 1H, 9-H), 3.30 (q, 1H, $J = 6.3$ Hz, 1″-H), 3.24 (brs, 1H, 16-H), 3.23 (d, 1H, $J = 19.4$ Hz, 10-H), 3.14 (m, 2H, 1″-H′, 6″-H), 3.03 (d, 1H, $J = 19.3$ Hz, 10-H′), 2.91 (d, 1H, $J = 18.7$ Hz, 6″-H′), 2.84 (s, 3H, NCH$_3$), 2.73 (brs, 2H, 7-H, 16-H′), 2.69 (m, 1H, 15-H), 2.60 (m, 1H, 15-H′), 2.11 (t, 2H, $J = 6.4$ Hz, 20′-H), 1.80 (quin, 3H, $J = 7.0$ Hz, 17′-H, 8-H), 1.68 (d, 1H, $J = 8.5$ Hz, 7-H′), 1.57 (quin, 2H, 6.3 Hz, 19′-H), [1.42 (m, 4H) and 1.26 (brs, 4H)] (2″-H, 3″-H, 4″-H, 5″-H), 1.34 (m, 1H, 8-H′), 1.26 (brs, 2H, 18′-H); ^{13}C NMR (126 MHz, CDCl$_3$) δ 192.4 (Ar-CO), 173.8 (20′-CONH), 170.0 (O-CH$_2$-$\underline{C}$ONH), 156.8 (C-6), 145.6 (C-4), 143.9 (C-3), 139.0 (C-8′), 138.3 (C-2′), 137.2 (C-7a′), 133.9 (C-11a′), 130.8 (C-15a′), 130.2 (C-11′), 128.4 (C-12′), 128.3 (C-12), 127.1 (C-3a′), 126.9 (C-14′), 126.5 (C-13′), 126.1 (C-9′), 126.0 (C-15′), 124.8 (C-10′), 123.9 (C-6′), 123.1 (C-5′), 123.0 (C-4′), 121.3 (C-11), 120.0 (C-1), 117.6 (C-3′), 116.0 (C-2), 110.2 (C-7′), 86.4 (C-5), 73.3 (O-$\underline{C}$H$_2$-CO), 70.4 (C-14), 66.0 (C-9), 56.9 (OCH$_3$), 47.6 (C-16), 47.1 (C-16′), 46.0 (C-13), 42.0 (NCH$_3$), 39.4 (C-6″), 38.7 (C-1″), 36.2 (C-20′), 29.5 (C-17′), (29.2, 28.3, 26.1, 26.0) (C-2″, C-3″, C-4″, C-5″), 29.0 (C-7), 28.4 (C-8), 26.4 (C-18′), 25.3 (C-19′), 24.0 (C-10), 17.9 (C-15); MALDI-MS calcd for C$_{51}$H$_{59}$N$_5$O$_7$ 853.44, found 854.49 [M+H]$^+$.

2.13. Bivalent compound 12

Prepared as described for **10**, but **7** (26.8 mg, 38 μmol) was used. Yield 11.1 mg of **12** (61%) as yellow oil. R$_f$ 0.70 (CHCl$_3$−MeOH 9:1); HPLC k' = 6.06 (t$_R$ = 14.8 min, linear gradient of 10 → 100% B in A over 25 min); ^{1}H NMR (500 MHz, CDCl$_3$) δ 8.42 (d, 1H, $J = 6.8$ Hz, 4′-H), 8.16 (d, 1H, $J = 8.3$ Hz, 15′-H), 7.97 (d, 1H, $J = 8.1$ Hz, 11′-H), 7.90 (d, 1H, $J = 8.1$ Hz, 12′-H), 7.65 (d, 1H, $J = 6.6$ Hz, 9′-H), 7.53 (t, 1H, $J = 7.6$ Hz, 10′-H), 7.51 (t, 1H, $J = 7.5$ Hz, 13′-H), 7.45 (t, 1H, $J = 7.3$ Hz, 14′-H), 7.40 and 7.39 (2 × s, 2 × 1H, 2′-H, 7′-H), 7.34 (m, 2H, 5′-H, 6′-H), 6.80 (d, 1H, $J = 8.2$ Hz, 2-H), 6.71 (d, 1H, $J = 8.3$ Hz, 1-H), 6.68 (brs, CONH), 6.55 (brs, CONH), 5.01 (s, 1H, 5-H), 4.59 and 4.50 (2 × d, 2 × 1H, $J = 15.9$ Hz, O-CH$_2$-CO), 4.09 (t, 2H, $J = 6.9$ Hz, 16′-H), 3.87 (s, 3H, OCH$_3$), 3.77 (brs, 1H, 9-H), 3.58−3.41 (m, 12H, 3″-H, 5″-H, 6″-H, 8″-H, 9″-H, 11″-H), 3.27 (brs, 4H, 1″-H, 13″-H), 3.26 (brs, 1H, 16-H), 3.22 (d, 1H, $J = 19.1$ Hz, 10-H), 3.03 (d, 1H, $J = 18.6$ Hz, 10-H′), 2.86 (s, 3H, NCH$_3$), 2.74 (brs, 2H, 7-H, 16-H′), 2.70 (brs, 1H, 15-H), 2.60 (d, 1H, $J = 12.0$ Hz, 15-H′), 2.12 (t, 2H, $J = 6.5$ Hz, 20′-H), 1.81 (m, 3H, 8-H, 17′-H), 1.70 (m, 5H, 7-H′, 2″-H, 12″-H), 1.59 (quin, 2H, 6.7 Hz, 19′-H), 1.37 (brs, 1H, 8-H′), 1.27 (m, 2H, 18′-H); ^{13}C NMR (126 MHz, CDCl$_3$) δ 192.3 (Ar-CO), 173.8 (20′-CONH), 169.9 (O-CH$_2$-$\underline{C}$ONH), 156.7 (C-6), 145.7 (C-4), 143.9 (C-3), 139.0 (C-8′), 138.2 (C-2′), 137.2 (C-7a′), 133.9 (C-11a′), 130.9 (C-15a′), 130.2 (C-11′), 128.4

(2C, C-12, C-12′), 127.1 (C-3a′), 126.9 (C-14′), 126.5 (C-13′), 126.1 (C-9′), 126.0 (C-15′), 124.8 (C-10′), 123.8 (C-6′), 123.05 (C-5′), 122.97 (C-4′), 121.3 (C-11), 119.9 (C-1), 117.6 (C-3′), 116.0 (C-2), 110.2 (C-7′), 86.5 (C-5), 73.3 (O-CH_2-CO), (70.3, 70.1, 70.0, 69.9, 69.4) (7C, C-14, C-3″, C-5″, C-6″, C-8″, C-9″, C-11″), 66.0 (C-9), 57.0 (OCH$_3$), 47.6 (C-16), 47.1 (C-16′), 46.1 (C-13), 42.0 (NCH$_3$), 38.1 and 37.1 (C-1″, C-13″), 36.1 (C-20′), 30.6 (C-8), 29.6 (C-17′), 29.2 (C-7), 28.9 (C-2″, C-12″), 26.4 (C-18′), 25.2 (C-19′), 24.1 (C-10), 17.8 (C-15); MALDI-MS calcd for $C_{55}H_{67}N_5O_{10}$ 957.49, found 958.23 [M+H]$^+$.

2.14. (1H-Indol-3-yl)(naphthalen-1-yl)methanone (13)

Indole (250 mg, 2.13 mmol) was dissolved in 5 mL of DCM and 1.74 mL of Et$_2$AlCl (25% (w/w) in toluene (3.2 mmol) was added at 0 °C. The mixture was stirred at 0 °C for 30 min and 1-naphthoyl chloride (609 mg, 3.2 mmol dissolved in 8 mL of DCM) was added dropwise to the solution at 0 °C, and it was stirred for 16 h. Then the reaction mixture was quenched with 100 mM NaHCO$_3$. The precipitate was filtered and the filtrate was evaporated in vacuo. The crude product was purified by column chromatography on silica gel 60 (n-hexane–EtOAc 2:1) to give 13 (406 mg, 70%) as yellow solid. R$_f$ 0.44 (n-hexane–EtOAc 2:1); ^{1}H NMR (300 MHz, CDCl$_3$) δ 8.73 (brs, 1H, NH indole), 8.50 (d, 1H, J = 6.6 Hz, 4-H), 8.17 (d, 1H, J = 8.1 Hz, 15′-H), 7.96 (d, 1H, J = 8.4 Hz, 11′-H), 7.89 (d, 1H, J = 7.5 Hz, 12′-H), 7.66 (d, 1H, J = 6.8 Hz, 9′-H), 7.53–7.36 (m, 7H, 10′-H, 13′-H, 14′-H, 2-H, 5-H, 6-H, 7-H); ^{13}C NMR (300 MHz, CDCl$_3$) δ 138.7, 136.5, 134.9, 133.7, 130.7, 130.1, 128.1, 126.8, 126.3, 125.9, 125.8, 124.5, 124.1, 123.0, 122.7, 119.2, 111.4; ESI-MS calcd for $C_{19}H_{13}NO$ 271.10, found 272.24 [M+H]$^+$.

2.15. tert-Butyl 5-bromopentylcarbamate (14)

To a stirred solution of tert-butyl 5-hydroxypentyl-carbamate (500 mg, 2.46 mmol) and TEA (498 mg, 4.92 mmol) in 5 mL DCM at −10 °C was added MsCl (338 mg, 2.95 mmol) dropwise and the solution was stirred at the same temperature for 5 h. The reaction was then quenched with water. The organic layer was washed with water, brine, dried over MgSO$_4$, filtered and evaporated under reduced pressure to give the desired product as yellow oil (552 mg, 80%, R$_f$ 0.5 (EtOAc)) The mesylate was used in the next step without any further purification. Under N$_2$ atmosphere 5-(tert-butoxycarbonylamino)pentyl methanesulfonate (350 mg, 1.2 mmol) was dissolved in 5 mL THF followed by the addition of LiBr (313 mg, 3.6 mmol) to the solution. The reaction mixture was stirred for 16 h under reflux, then THF was removed under vacuum. The mixture was diluted with 10 mL water and it was extracted with DCM (3 × 10 mL). The combined organic phase was washed with water (3 × 10 mL) and brine (3 × 10 mL), dried over MgSO$_4$ and evaporated in vacuo. The product was purified by column chromatography on silica gel 60 (n-hexane–EtOAc 9:1) to give white crystalline product (230 mg, 72%). R$_f$ 0.6 (n-hexane–EtOAc 4:1); ^{1}H NMR (300 MHz, CDCl$_3$) δ 4.59 (brs, 1H, NH), 3.37 (t, 2H, J = 8.4 Hz, 5-H), 3.09 (q, 2H, J = 7.8 Hz, 1-H), 1.84 (quin, 2H, J = 7.3 Hz, 4-H), 1.49–1.36 (m, 4H, 2-H, 3-H), 1.40 (s, 9H, CH$_3$); ^{13}C NMR (300 MHz, CDCl$_3$) δ 155.9 (CONH), 79.0 ($\underline{C}$(CH$_3$)$_3$), 40.2 (C-1), 33.6 (C-5), 32.2 (C-4), 29.2 (CH$_3$), 28.3 (C-2), 25.3 (C-3); ESI-MS calcd for $C_{10}H_{20}BrNO_2$ 265.07, found 266.12 [M+H]$^+$.

2.16. tert-Butyl (5-(3-(1-naphthoyl)-1H-indol-1-yl)pentyl)carbamate (15)

To a stirred solution of NaH (60% dispersion in mineral oil, 15.4 mg, 0.44 mmol) in 5 mL of DMF at 0 °C was added 13 (100 mg, 0.368 mmol) in 10 mL DMF dropwise and the mixture was stirred at 80 °C for 1 h. The reaction mixture was cooled to 0 °C and a solution of 14 (108 mg, 0.41 mmol) in 5 mL DMF was added dropwise and stirred at 0 °C for 30 min, and then stirred for 18 h at rt. Then it was evaporated and the oily residue was dissolved in EtOAc (50 mL). The organic layer was washed with water (3 × 50 mL) and brine (3 × 50 mL), dried over Na$_2$SO$_4$ and evaporated in vacuo. The crude residue was purified by column chromatography on silica gel 60 (ethyl acetate/hexane 1:2) to yield 15 (142 mg, 85%) as orange-red oil. R$_f$ 0.59 (n-hexane–EtOAc 2:1); HPLC k' = 6.36 (t$_R$ = 20.6 min, linear gradient of 5 → 95% B in A over 25 min); ^{1}H NMR (300 MHz, DMSO-d_6) δ 8.29 (d, 1H, J = 8.4 Hz, 15′-H), 8.07 (d, 1H, J = 8.1 Hz, 11′-H), 8.00 (t, 1H, 14′-H), 7.75 (s, 1H, 2′-H), 7.68–7.49 (m, 5H, 9′-H, 7′-H, 13′-H, 10′-H, 12′-H), 7.30 (m, 2H, 5′-H, 6′-H), 6.72 (t, 1H, NH-Boc), 4.17 (t, 2H, J = 7.3 Hz, 1′-H), 2.81 (q, 2H, 5′-H), 1.68 (quin, 2H, J = 7.3 Hz, 2′-H), 1.29–1.15 (m, 13H, 4′-H, 3′-H, 3 × CH$_3$); ^{13}C NMR (300 MHz, DMSO-d_6) δ 191.3 (3-CO), 155.9 (CONH), 139.8 (C-8′), 138.9 (C-2), 137.2 (C-7a), 133.7 (C-11a′), 130.5 (C-15a′), 130.1 (C-11′), 128.7 (C-12′), 127.1 (C-14′), 126.8 (C-3a), 126.7 (C-13′), 126.2 (C-9′), 125.7 (C-15′), 125.4 (C-10′), 123.7 (C-6), 122.9 (C-4), 122.1 (C-5), 116.4 (C-3), 111.5 (C-7), 77.7 ($\underline{C}$(CH$_3$)$_3$), 46.6 (C-1′), 29.5 (C-4′), 29.3 (C-2′), 28.6 (CH$_3$), 23.7 (C-3′); ESI-MS calcd for $C_{29}H_{32}N_2O_3$ 456.24, found 457.12 [M+H]$^+$.

2.17. (1-(5-Aminopentyl)-1H-indol-3-yl)(naphthalen-1-yl)methanone (16)

The Boc-protected amine 15 (137 mg, 0.3 mmol) was dissolved in 2 mL DCM containing 50% (v/v) TFA and it was stirred for 30 min at rt. The solution was evaporated and the product was washed with DCM and evaporated in vacuo to give 16 (135 mg, 97%); R$_f$ 0.56 (MeOH–AcOH 95:5); HPLC k' = 4.22 (t$_R$ = 11.0 min, linear gradient of 10 → 100% B in A over 25 min); ESI-MS calcd for $C_{24}H_{24}N_2O$ 356.19, found 357.08 [M+H]$^+$.

2.18. N-(5-(3-(1-Naphthoyl)-1H-indol-1-yl)pentyl)acetamide (17)

The amine 16 (17 mg, 36 μmol) dissolved in 1 mL of DCM followed by the addition of 0.3 mL TEA and 0.3 mL acetic anhydride. The mixture was then stirred at rt for 16 h, then it was evaporated in vacuo. The crude 17 was purified by column chromatography on silica gel 60 (EtOAc–DCM 9:1) to give 17 (13 mg, 91%); R$_f$ 0.54 (n-hexane–EtOAc 2:1); HPLC k' = 4.70 (t$_R$ = 16.0 min, linear gradient of 20 → 100% B in A over 25 min); ^{1}H NMR (300 MHz, DMSO-d_6) δ 8.31 (d, 1H, 15′-H), 8.06 (d, 1H, J = 8.1 Hz, 11′-H), 8.00 (d, 1H, J = 8.2 Hz, 14′-H), 7.76 (s, 1H, 2′-H), 7.74–7.48 (m, 6H, 9′-H, 7′-H, 13′-H, 10′-H, 12′-H, NH), 7.30 (m, 2H, 5′-H, 6′-H), 4.17 (t, 2H, J = 7.3 Hz, 1′-H), 2.93 (q, 2H, J = 5.7 Hz, 5′-H), 1.71–1.65 (m, 5H, CH$_3$ and 2′-H), 1.32 (quin, 2H, J = 7.3 Hz, 4′-H), 1.17 (quin, 2H, J = 7.4 Hz, 3′-H); ^{13}C NMR (300 MHz, DMSO-d_6) δ 191.3 (3-CO), 169.3 (CONH), 139.8 (C-8′), 138.9 (C-2), 137.2 (C-7a), 133.7 (C-11a′), 130.5 (C-15a′), 130.1 (C-11′), 128.7 (C-12′), 127.1 (C-14′), 126.8 (C-3a), 126.7 (C-13′), 126.2 (C-9′), 125.7 (C-15′), 125.4 (C-10′), 123.7 (C-6), 122.9 (C-4), 122.2 (C-5), 116.4 (C-3), 111.5 (C-7), 46.5 (C-1′), 38.6 (C-5′), 29.6 (C-4′), 29.0 (C-2′), 23.9 (CH$_3$), 23.01 (C-3′); ESI-MS calcd for $C_{26}H_{26}N_2O_2$ 398.20, found 399.02 [M+H]$^+$.

2.19. Peptide synthesis, general procedure

To an ice-cooled mixture containing N-protected amino acid or peptide (0.28 mmol) in DCM (5 mL), EDC.HCl (1.1 equiv., 0.28 mmol), HOBt (1.1 equiv., 0.28 mmol), NMM (3.3 equiv., 0.85 mmol), the required protected amino acid (1 equiv., 0.25 mmol) dissolved in DMF (2.5 mL) was added. The reaction mixture was allowed to warm at rt for 16 h and evaporated under reduced pressure. The residue was then dissolved in EtOAc and washed with three portions of 5% citric acid, NaHCO$_3$ and brine. The

organic phase was dried over Na_2SO_4, and the solvent evaporated under reduced pressure to give the desired product. All final Boc-protected intermediates have been purified by flash chromatography on silica gel 60 and then treated with a mixture of TFA/DCM (1:1) for 30 min at ambient temperature. The final products as TFA salts were lyophilised and then characterized as follows.

2.20. Tyr-D-Ala-Gly-Phe-NH₂

It was prepared as described [44].

2.21. Bivalent compound 18

Overall isolated yield 21%; R_f 0.71 (ACN−MeOH−H₂O 4:1:1); HPLC k' = 4.43 (t_R = 15.2 min, linear gradient of 20 → 100% B in A over 25 min); ¹H NMR (300 MHz, DMSO-d_6) δ 9.34 (s, 1H, Tyr OH), 8.57 (d, 1H, J = 6.9 Hz, D-Ala NH), 8.28 (d, 1H, J = 7.2 Hz, 15′-H), 8.20 (t, 1H, Gly NH), 8.08−7.94 (m, 8H, Phe ArH, Tyr NH, Phe NH, 5′-NH), 7.74 (s, 1H, 2-H), 7.66−7.44 (m, 5H, 9′-H, 10′-H, 11′-H, 12′-H, 13′-H), 7.33 (quin, 1H, 14′-H), 7.21−7.09 (m, 4H, 4-H, 5-H, 6-H, 7-H), 7.01 (d, 2H, J = 8.7 Hz, Tyr ArH), 6.68 (d, 2H, J = 8.7 Hz, Tyr ArH), 4.41 (q, 1H, Phe H^α), 4.28 (quin, 1H, D-Ala H^α), 4.15 (t, 2H, 1′-H), 3.95 (q, 1H, Tyr H^α), 3.61 (dd, 2H, Gly H^α), 2.97−2.67 (m, 6H, Phe H^β, Tyr H^β, 5′-H), 1.65 (quin, 2H, 2′-H), 1.25 (quin, 2H, 4′-H) 1.10−1.02 (m, 5H, 3′-H, D-Ala H^β); ESI-MS calcd for $C_{47}H_{50}N_6O_6$ 794.38, found 795.63 $[M+H]^+$.

2.22. Bivalent compound 19

Overall isolated yield 14%; R_f 0.73 (ACN−MeOH−H₂O 4:1:1); HPLC k' = 4.24 (t_R = 14.7 min, linear gradient of 20 → 100% B in A over 25 min); ¹H NMR (300 MHz, DMSO-d_6) δ 9.30 (s, 1H, Tyr OH), 8.49 (d, 1H, J = 6.9 Hz, D-Ala NH), 8.27 (m, 2H, Gly NH, 15′-H), 8.18 (t, 1H, Gly NH), 8.07−7.96 (m, 6H, 9′-H, 10′-H, 11′-H, 12′-H, 13′-H, Tyr NH, Phe NH), 7.87 (brs, 1H, Tyr NH), 7.75 (s, 1H, 2-H), 7.65−7.48 (m, 5H, 4-H, 5-H, 6-H, 7-H, 5′-NH), 7.29 (m, 1H, 14′-H), 7.19−7.13 (m, 5H, Phe ArH), 6.98 (d, 2H, J = 8.7 Hz, Tyr ArH), 6.66 (d, 2H, J = 8.7 Hz, Tyr ArH), 4.47 (q, 1H, Phe H^α), 4.27 (quin, 1H, D-Ala H^α), 4.16 (t, 2H, 1′-H), 3.91 (q, 1H, Tyr H^α), 3.56 (d, 4H, Gly H^α), 2.96−2.70 (m, 6H, 5′-H, Tyr H^β, Phe H^β), 1.68 (quin, 2H, 2′-H), 1.36 (quin, 2H, 4′-H), 1.18 (quin, 2H, 3′-H), 1.01 (d, 3H, D-Ala H^β); ESI-MS calcd for $C_{49}H_{53}N_7O_7$ 851.40, found 852.63 $[M+H]^+$.

2.23. Bivalent compound 20

Overall isolated yield 25%; R_f 0.68 (ACN−MeOH−H₂O 4:1:1); HPLC k' = 6.59 (t_R = 15.9 min, linear gradient of 5 → 95% B in A over 25 min); ¹H NMR (300 MHz, DMSO-d_6) δ 9.33 (s, 1H, OH Tyr), 8.55 (d, 1H, D-Ala NH), 8.28 (d, 1H, 15′-H), 8.20 (t, 1H, Gly NH), 8.09−7.97 (m, 9H, Phe ArH, Phe NH, β-Ala NH, Tyr NH, 5′-NH), 7.77−7.49 (m, 7H, 2-H, 9′-H, 10′-H, 11′-H, 12′-H, 13′-H, 14′-H), 7.34−7.12 (m, 4H, 4-H, 5-H, 6-H, 7-H), 7.01 (d, 2H, Tyr ArH), 6.68 (d, 2H, Tyr ArH), 4.39 (q, 1H, Phe H^α), 4.29 (quin, 1H, D-Ala H^α), 4.16 (t, 2H, 1′-H), 3.95 (q, 1H, Tyr H^α), 3.58 (d, 2H, Gly H^α), 2.93−2.71 (m, 6H, 5′-H, Tyr H^β, Phe H^β), 2.13 (t, 2H, βAla H^α), 1.67 (quin, 2H, 2′-H), 1.33 (quin, 2H, 4′-H), 1.21−1.15 (m, 4H, β-Ala H^β, 3′-H), 1.05 (d, 3H, D-Ala H^β); ESI-MS calcd for $C_{50}H_{55}N_7O_7$ 865.42, found 866.14 $[M+H]^+$.

2.24. Bivalent compound 21

Overall isolated yield 12%; R_f 0.67 (ACN−MeOH−H₂O 4:1:1); HPLC k' = 4.27 (t_R = 14.8 min, linear gradient of 20 → 100% B in A over 25 min); ¹H NMR (300 MHz, DMSO-d_6) δ 9.32 (s, 1H, Tyr OH), 8.54 (d, 1H, D-Ala NH), 8.29 (d, 1H, 15′-H), 8.20 (t, 1H, Gly NH), 8.06−8.00 (m, 8H, Phe ArH, Phe NH, Tyr NH, 5′-NH), 7.75 (s, 1H, 2-

H), 7.63−7.52 (m, 6H, 12′-H, 9′-H, 10′-H, 11′-H, 14′-H, 13′-H), 7.30−7.11 (m, 4H, 4-H, 5-H, 6-H, 7-H), 6.96 (d, 2H, Tyr ArH), 6.69 (d, 2H, Tyr ArH), 4.40 (q, 1H, Phe H^α), 4.29 (quin, 1H, D-Ala H^α), 4.18 (t, 2H, 1′-H), 3.96 (q, 1H, Tyr H^α), 3.64 (d, 2H, Gly H^α), 2.94−2.70 (m, 7H, Tyr H^β, Phe H^β, Gaba NH, 5′-H), 1.93 (t, 2H, Gaba H^α), 1.69 (quin, 2H, J = 7.3 Hz, 2′-H), 1.49 (quin, 2H, Gaba H^β), 1.33 (quin, 2H, 4′-H), 1.21 (m, 4H, 3′-H, Gaba H^γ), 1.06 (d, 3H, D-Ala H^β); ESI-MS calcd for $C_{51}H_{57}N_7O_7$ 879.43, found 880.23 $[M+H]^+$.

2.25. 1-Pentyl-1H-indole (22)

To a stirred solution of indole (1.17 g, 10 mmol) in ACN (10 mL) were added TEA (1.01 g, 10 mmol) and 1-iodopentane (1.98 g, 10 mmol), then the solution was stirred at 80 °C for 16 h. The solvent was evaporated in vacuo and the residue was extracted with water and CHCl₃ (3 × 20 mL). The combined organic phase was washed with brine, and dried over Na_2SO_4. After evaporation the crude product was purified by column chromatography (n-hexane−EtOAc 95:5) to give 1.40 g (75%) of pure 22 as an oil. R_f 0.70 (n-hexane−EtOAc 95:5); HPLC k' = 4.30 (t_R = 11.7 min, linear gradient of 50 → 100% B in A over 25 min); ¹H NMR (500 MHz, CDCl₃) δ 7.63 (d, 1H, J = 7.9 Hz, 4-H), 7.35 (d, 1H, J = 8.1 Hz, 7-H), 7.20 (t, 1H, J = 7.6 Hz, 5-H), 7.10 (d, 1H, J = 3.1 Hz, 2-H), 7.09 (t, 1H, J = 8.0 Hz, 6-H), 6.49 (d, 1H, J = 3.1 Hz, 3-H), 4.12 (t, 2H, J = 7.2 Hz, 1′-H), 1.85 (quin, 2H, J = 7.2 Hz, 2′-H), 1.33 (m, 4H, 3′-H, 4′-H), 0.89 (t, 3H, J = 7.0 Hz, CH₃); ¹³C NMR (126 MHz, CDCl₃) δ 136.1 (C-7a), 128.7 (C-3a), 127.9 (C-2), 121.4 (C-6), 121.1 (C-4), 119.3 (C-5), 109.5 (C-7), 100.9 (C-3), 46.6 (C-1′), 30.1 (C-2′), 29.3 (C-3′), 22.5 (C-4′), 14.1 (CH₃); ESI-MS calcd for $C_{13}H_{17}N$ 187.14, found 188.02 $[M+H]^+$.

2.26. 5-Bromo-1-pentyl-1H-indole (23)

1.96 g of 5-bromo-1H-indole (10 mmol) was dissolved in 20 mL of DMF containing 1.6 g of powdered NaOH, then 1-iodopentane (1.98 g, 10 mmol) was added dropwise. After 4 h stirring at ambient temperature the mixture was filtered and the filtrate was evaporated in vacuo. The resulting oil was dissolved in CHCl₃ and extracted with water. The organic phase was washed with brine and dried over Na_2SO_4. The crude product was purified by column chromatography (n-hexane−EtOAc 95:5) to give 1.75 g (66%) of pure 23 as an oil. R_f 0.62 (n-hexane−EtOAc 95:5); HPLC k' = 6.18 (t_R = 15.8 min, linear gradient of 50 → 100% B in A over 25 min); ¹H NMR (CDCl₃) ¹H NMR (500 MHz, CDCl₃) δ 7.74 (d, 1H, J = 1.6 Hz, 4-H), 7.27 (dd, 1H, J = 8.8 Hz, 1.6 Hz, 7-H), 7.21 (d, 1H, J = 8.8 Hz, 6-H), 7.09 (d, 1H, J = 3.0 Hz, 2-H), 6.42 (d, 1H, J = 2.9 Hz, 3-H), 4.08 (t, 2H, J = 7.2 Hz, 1′-H), 1.82 (quin, 2H, J = 7.3 Hz, 2′-H), 1.31 (m, 4H, 3′-H, 4′-H), 0.88 (t, 3H, J = 7.1 Hz, CH₃); ¹³C NMR (126 MHz, CDCl₃) δ 134.8 (C-7a), 130.3 (C-3a), 129.1 (C-2), 124.3 (C-6), 123.5 (C-4), 112.6 (C-5), 111.0 (C-7), 100.6 (C-3), 46.7 (C-1′), 30.1 (C-2′), 29.2 (C-3′), 22.4 (C-4′), 14.1 (CH₃); ESI-MS calcd for $C_{13}H_{16}BrN$ 265.05, found 266.18 $[M+H]^+$.

2.27. Naphthalen-1-yl(1-pentyl-1H-indol-3-yl)methanone (24)

To a stirred solution of 22 (281 mg, 1.5 mmol) in 10 mL of dry DCM at 0 °C was added dropwise 1.5 mL of 1 M Et₂AlCl in hexane (1.5 mmol). The solution was stirred at 0 °C for 1 h followed by the dropwise addition of 286 mg of 1-naphthoyl chloride (1.5 mmol) in 3 mL DCM. The reaction mixture was stirred at 0 °C for 16 h then the solution was poured carefully into a mixture of ice and 0.1 M HCl and it was extracted with DCM. The combined organic phase was evaporated and the residue was dissolved in diethyl ether that was washed with 15% K₂CO₃. The organic phase was evaporated and the crude product was purified by column chromatography (n-hexane−EtOAc 4:1) to give 368 mg (72%) of pure 24 as an oil. R_f 0.44 (n-

hexane–EtOAc 4:1); HPLC k' = 8.08 (t_R = 19.1 min, linear gradient of 50 → 95% B in A over 25 min); ^{1}H NMR (500 MHz, CDCl$_3$) δ 8.49 (m, 1H, 4-H), 8.19 (d, 1H, J = 8.4 Hz, 15'-H), 7.97 (d, 1H, J = 8.2 Hz, 11'-H), 7.91 (d, 1H, J = 8.1 Hz, 12'-H), 7.66 (d, 1H, J = 6.9 Hz, 9'-H), [7.53 (t, 1H, J = 7.5 Hz) and 7.52 (t, 1H, J = 7.1 Hz)] (10'-H and 13'-H), 7.47 (t, 1H, J = 7.6 Hz, 14'-H), 7.41–7.35 (overlapping m, 4H, 2-H, 5-H, 6-H, 7-H), 4.07 (t, 2H, J = 7.3 Hz, 1'-H), 1.81 (quin, 2H, J = 7.4 Hz, 2'-H), 1.28 (m, 4H, 3'-H, 4'-H), 0.85 (t, 3H, J = 7.0 Hz, CH$_3$); ^{13}C NMR (126 MHz, CDCl$_3$) δ 192.2 (CO), 139.3 (C-8'), 138.1 (C-2), 137.2 (C-7a), 133.9 (C-11a'), 131.0 (C-15a'), 130.1 (C-11'), 128.3 (C-12'), 127.2 (C-3a), 126.9 (C-14'), 126.4 (C-13'), 126.2 (C-9'), 126.0 (C-15'), 124.7 (C-10'), 123.7 (C-6), 123.1 (C-5), 123.0 (C-4), 117.7 (C-3), 110.1 (C-7), 47.3 (C-1'), 29.6 (C-2'), 29.1 (C-3'), 22.3 (C-4'), 14.0 (CH$_3$); ESI-MS calcd for C$_{24}$H$_{23}$NO 341.18, found 341.95 [M+H]$^+$.

2.28. Naphthalen-1-yl(5-bromo-1-pentyl-1H-indol-3-yl) methanone (25)

Prepared as described for **24**, but starting from **23** (400 mg, 1.5 mmol). The crude product was purified by column chromatography (n-hexane–EtOAc 4:1) to give 517 mg (82%) of pure **25** as an oil. R$_f$ 0.40 (n-hexane–EtOAc 4:1); HPLC k' = 7.62 (t_R = 18.1 min, linear gradient of 50 → 100% B in A over 25 min); ^{1}H NMR (500 MHz, CDCl$_3$) δ 8.71 (d, 1H, J = 1.6 Hz, 4-H), 8.17 (d, 1H, J = 8.3 Hz, 15'-H), 7.98 (d, 1H, J = 8.2 Hz, 11'-H), 7.92 (d, 1H, J = 8.0 Hz, 12'-H), 7.65 (dd, 1H, J = 6.9 Hz, 0.7 Hz, 9'-H), [7.53 (t, 1H, J = 7.6 Hz) and 7.52 (t, 1H, J = 6.7 Hz)] (10'-H and 13'-H), 7.48 (dt, 1H, J = 7.7 Hz, 1.2 Hz, 14'-H), 7.45 (dd, 1H, J = 8.7 Hz, 1.8 Hz, 6-H), 7.32 (s, 1H, 2-H), 7.26 (d, 1H, J = 8.4 Hz, 7-H), 4.04 (t, 2H, J = 7.2 Hz, 1'-H), 1.79 (quin, 2H, J = 7.4 Hz, 2'-H), 1.26 (m, 4H, 3'-H, 4'-H), 0.85 (t, 3H, J = 7.1 Hz, CH$_3$); ^{13}C NMR (126 MHz, CDCl$_3$) δ 191.9 (CO), 138.8 (C-8'), 138.5 (C-2), 135.9 (C-7a), 133.9 (C-11a), 130.9 (C-15a), 130.4 (C-11'), 128.7 (C-3a), 128.4 (C-12'), 127.0 (C-14'), 126.8 (C-13'), 126.5 (C-9'), 126.0 (2C, C-15', C-6), 125.8 (C-4), 124.7 (C-10'), 117.2 (C-3), 116.8 (C-5), 111.5 (C-7), 47.5 (C-1'), 29.6 (C-2'), 29.0 (C-3'), 22.3 (C-4'), 14.0 (CH$_3$); ESI-MS calcd for C$_{24}$H$_{22}$BrNO 419.09, found 420.14 [M+H]$^+$.

2.29. [^{3}H]Naphthalen-1-yl(1-pentyl-1H-indol-3-yl)methanone (26)

Tritium labeling was performed with 3.6 mg of **25** (8.5 μmol) dissolved in 0.6 mL of EtOAc in the presence of 3 mg of Pd/C (10% Pd) catalyst and triethylamine (1.5 μL, 10.7 μmol). The reaction mixture was degassed prior to tritium reduction by two freeze-thaw cycles, and then it was stirred under 0.25 bar of tritium gas for 4 h at rt. The unreacted tritium gas was then adsorbed onto pyrophoric uranium and the catalyst was filtered off with a syringe filter. The filtrate was evaporated in vacuo and the labile tritium was removed by repeated evaporations from EtOH solution. Finally 7.03 GBq of [^{3}H]JWH-018 was isolated as a white solid that was purified by HPLC on a Phenomenex Luna C18(2) column (k' = 8.08 (t_R = 19.1 min), linear gradient of 50 → 95% B in A over 25 min). The specific activity was determined by using an HPLC peak area calibration curve recorded with **24** and it was found to be 1.48 TBq/mmol. The tritium labeled JWH-018 was dissolved in EtOH (37 MBq/mL) and stored under liquid nitrogen.

2.30. Tritium labeling of 11

2 mL 1.15 mg/mL MeOH solution of **9** (6 μmol) was mixed with 250 μL 3% (v/v) ICl in MeOH (14.2 μmol) and the solution was stirred at ambient temperature for 60 min. Then 50 mg/mL Na$_2$S$_2$O$_5$ in water was added until decolorization, and the iodo derivative of **9** was purified by semipreparative HPLC on a Phenomenex Luna C18(2) stationary phase. The resulting 1.6 mg (55%) of iodo-**9** was dissolved in 400 μL DMF and 3 mg of Pd/BaSO$_4$ (10% Pd) catalyst and

triethylamine (1.4 μL, 10 μmol) were added and tritium labeling was performed as described for [^{3}H]JWH-018 to give 64 MBq of [^{3}H]**9** with a specific activity of 64 GBq/mmol. Finally, 37 MBq of [^{3}H]**9** and HOBt.H$_2$O (0.3 mg, 1.9 μmol) were dissolved in 150 μL of DMF and DIC (0.3 μL, 1.9 μmol) was added. It was stirred for 5 min, then **6** (2.1 mg, 2.9 μmol) and DIEA (1.4 μL, 8 μmol) were added and the solution was stirred at rt for 16 h. It was then evaporated in vacuo and the crude product was purified by HPLC on a Phenomenex Luna C18(2) column that yielded 5.5 MBq [^{3}H]**11** (15%). S.a. 64 GBq/mmol; HPLC k' = 5.48 (t_R = 13.6 min, linear gradient of 20 → 100% B in A over 25 min).

2.31. Tritium labeling of 19

To a solution of **19** (970 μL 1 mg/mL MeOH, 1 μmol) 1.8 mg of IPy$_2$BF$_4$ (4.8 μmol) and 4.4 μL of HBF$_4$ in Et$_2$O were added and the reaction mixture was stirred for 1 h at rt under nitrogen. The reaction was quenched with a solution of Na$_2$S$_2$O$_5$ in water and the iodo derivative of **19** was purified by HPLC on a Phenomenex Luna C18(2) stationary phase yielding 0.8 mg (60%) of diiodo-**19**. It was dissolved in 400 μL DMF and 2.5 mg of Pd/BaSO$_4$ (10% Pd) catalyst and triethylamine (0.8 μL, 5.6 μmol) were added and tritium labeling was performed as described for [^{3}H]JWH-018 to give 80 MBq of [^{3}H]**19** with a specific activity of 185 GBq/mmol. HPLC k' = 6.78 (t_R = 16.3 min, linear gradient of 5 → 95% B in A over 25 min).

2.32. Preparation of brain membrane homogenates

Wistar rats and guinea pigs were locally bred and handled according to the EU Directive 2010/63/EU and to the Regulations on Animal Protection (40/2013. (II. 14.) Korm. r.) of Hungary. Crude membrane fractions were prepared from the brain without cerebellum. Brains were quickly removed from the euthanized animals and directly put in ice-cold 50 mM Tris-HCl (pH 7.4) buffer. The collected tissue was then homogenized in 30 vol (v/w) of ice-cold buffer with a Braun Teflon-glass homogenizer at the highest rpm. The homogenate was centrifuged at 20 000×g for 25 min and the resulting pellet was suspended in the same volume of cold buffer followed by incubation at 37 °C for 30 min to remove endogenous ligands. After centrifugation the pellets were taken up in five volumes of 50 mM Tris-HCl (pH 7.4) buffer containing 0.32 M sucrose and stored in aliquots at −80 °C. Prior to the experiment, aliquots were thawed and centrifuged at 20 000×g for 25 min and the pellets were resuspended in 50 mM Tris-HCl (pH 7.4), homogenized with a Dounce followed by the determination of the protein content by the method of Bradford. The membrane suspensions were immediately used either in radioligand binding experiments or in [^{35}S]GTPγS functional assays.

2.33. Radioligand binding assays

Binding experiments of [^{3}H]JWH-018 were performed at 30 °C for 60 min in 50 mM Tris-HCl binding buffer (pH 7.4) containing 2.5 mM EGTA, 5 mM MgCl$_2$ and 0.5 mg/mL fatty acid free BSA in plastic tubes in a total assay volume of 1 mL that contained 0.3–0.5 mg/mL membrane protein. Association time course of [^{3}H]JWH-018 binding was obtained by incubating 0.6 nM [^{3}H]JWH-018 with rat brain membrane (0.45 mg/mL protein) at 30 °C for various periods of time (0–90 min) in the absence or presence of 10 μM JWH-018 to assess specific binding. Dissociation time course of [^{3}H]JWH-018 was obtained by incubating 0.6 nM [^{3}H]JWH-018 with rat brain membrane (0.45 mg/mL protein) at 30 °C for 60 min, then dissociation was initiated by the addition of 10 μM JWH-018 after different periods of incubation time. The kinetic equilibrium dissociation constant K$_d$ for [^{3}H]JWH-018 in rat brain membrane

homogenate was calculated as $K_d = k_d/k_a$, where k_d is the dissociation rate constant, k_a is the association rate constant calculated as $k_a = (k_{obs} - k_d)/[[^3H]JWH-018]$, k_{obs} is the observed pseudo-first order rate constant. Saturation binding experiments were performed by measuring the specific binding of $[^3H]$JWH-018 (0.5–35 nM) to rat brain membranes to determine the equilibrium dissociation constant (K_d) and the maximal number of binding sites (B_{max}). The specific binding was measured in the presence of 10 μM JWH-018.

Competition binding experiments were carried out by incubating brain membranes with opioid or cannabinoid receptor specific tritiated radioligands in the presence of increasing concentrations (10^{-11}–10^{-5} M) of various competing unlabeled ligands. MOR competition experiments were performed at 25 °C for 60 min with 2 nM $[^3H]$DAMGO ($K_d = 0.5$ nM), DOR competition experiments were performed at 35 °C for 45 min with 3 nM $[^3H]$Ile^{5,6}-deltorphin-2 ($K_d = 2.0$ nM) and KOR competition experiments were performed at 25 °C for 30 min with 1 nM $[^3H]$HS-665 ($K_d = 0.64$ nM) in 50 mM Tris-HCl binding buffer (pH 7.4) using rat brain (MOR, DOR) or guinea pig brain membrane homogenate (KOR). Non-specific binding was determined in the presence of 10 μM naloxone (MOR, DOR) or HS-665 (KOR). CB receptor binding experiments were performed at 30 °C for 60 min on rat brain membrane homogenates with 0.6 nM $[^3H]$JWH-018 ($K_d = 6.5$ nM) or with 1.5 nM $[^3H]$WIN-55,212−2 ($K_d = 10.1$ nM). Non-specific binding was determined in the presence of 10 μM JWH-018 or WIN-55,212−2. The competition experiments were terminated by diluting the suspensions with ice-cold wash buffer (50 mM Tris-HCl, 2.5 mM EGTA, 5 mM MgCl$_2$, 0.5% fatty acid free BSA, pH 7.4 for cannabinoid binding, or 50 mM Tris-HCl, pH 7.4 for opioid binding) followed by rapid washing and rapid filtration through Whatman GF/B or GF/C (MOR, KOR) glass fiber filters (Whatman Ltd, Maidstone, England) presoaked with 0.1% polyethyleneimine (only for CB receptor binding). Filtration was performed with a 24-well Brandel Cell Harvester (Gaithersburg, MD, USA). Filters were air-dried and immersed into Ultima Gold MV scintillation cocktail and then radioactivity was measured with a TRI-CARB 2100 TR liquid scintillation analyser (Packard).

2.34. Ligand stimulated [^{35}S]GTPγS binding assay

Rat brain membranes (30 μg protein/tube) were incubated with 0.05 nM [^{35}S]GTPγS (PerkinElmer) and 10^{-10}–10^{-5} M unlabeled ligands in the presence of 30 μM GDP, 100 mM NaCl, 3 mM MgCl$_2$ and 1 mM EGTA in 50 mM Tris-HCl buffer (pH 7.4) for 60 min at 30 °C. Basal [^{35}S]GTPγS binding was measured in the absence of ligands and set as 100%. Nonspecific binding was determined by the addition of 10 μM unlabeled GTPγS and subtracted from total binding. Incubation, filtration and radioactivity measurement of the samples were carried out as described above.

2.35. Cell culture and permeability assay

Primary rat brain endothelial cells, pericytes and astroglia cells were isolated and cultured according to the method described in our previous studies [45,46]. To induce BBB characteristics the isolated cells were co-cultured with the help of 12-well tissue culture inserts (Transwell, polycarbonate membrane, 3 μm pore size, Corning Costar, USA). After two days of co-culture brain endothelial cells became confluent and 550 nM hydrocortisone (Sigma) was added to the culture medium and one day before the experiment cells were treated with CPT-cAMP (250 mM, Sigma) and RO 201724 (17.5 mM; Sigma) for 24 h to tighten junctions and elevate transendothelial resistance [47]. Permeability tests on the co-cultured BBB model were performed when transendothelial electrical resistance values expressed to the surface area of the inserts reached 123.8 ± 12.9 Ωcm^2, n = 16. The resistance of cell-free inserts was subtracted from the measured data. During the permeability assay the culture medium was changed with the same as used in the growth period, but it also contained 10% serum. Compounds [^3H]**11** and [^3H]**19** were applied in the upper compartment in a final concentration of 0.25 and 0.75 μM. Compound permeability was measured from the A-B (from blood to brain) direction. After 15, 30 and 60 min samples were collected both from the upper and lower compartments and the transport of [^3H]**11** and [^3H]**19** was determined by measuring the radioactivity using a TRI-CARB 2100 TR liquid scintillation analyser (Packard). Flux of the compounds across coated, cell-free inserts was also measured. Endothelial permeability coefficients (P_e) were calculated from clearance values of [^3H]**11** and [^3H]**19** as described previously [47].

2.36. Hot plate test

Thermal nociception in the hot plate test was assessed with a commercially available apparatus consisting of a metal plate 25×25 cm (Ugo Basile, Italy) heated to a constant temperature of 55.0 ± 0.1 °C, on which a plastic cylinder (20 cm diameter, 18 cm high) was placed. The time of latency (s) was recorded from the moment the animal was placed in the cylinder on the hot plate until it licked its paws or jumped; the cut-off time was 60 s. The baseline was calculated as the mean of three readings recorded before testing at intervals of 15 min. The time course of latency was then determined at 15, 30, 45, 60, 90 and 120 min after compound treatment. Data were analysed as time-course curves of the percentage of maximum effect (%MPE= (post drug latency − baseline latency)/(cut-off time − baseline latency) × 100). CD-1 male mice (Harlan, Italy) weighing 25 g were used for the hot plate test. The research protocol was approved by the Service for Biotechnology and Animal Welfare of the Istituto Superiore di Sanità and authorized by the Italian Ministry of Health, according to Legislative Decree 26/14, which implemented the EU Directive 2010/63/EU on the protection of laboratory animals in Italy. Bivalent compounds **11** and **19** were injected intravenously (i.v.) at the dose of 10 mg/kg in a volume of 10 mL/kg. The control animals were injected i.v. with the vehicle of the compounds (physiological saline containing 5% DMSO, 10 mL/kg).

2.37. Nociceptive test in rats at spinal level

The procedures involved in the animal surgery and testing were approved by the Institutional Animal Care Committee of the University of Szeged, Faculty of Medicine. Surgical procedures including intrathecal (i.t.) catheterization and the monosodium iodoacetate (MIA)-induced inflammation are described in Supporting Information. Mechanical allodynia (von Frey test) was determined using a dynamic plantar aesthesiometer (Ugobasile, Comerio, Italy). Prior to baseline testing, each rat was habituated to a testing box with a wiremesh grid floor for 20 min. Straight metal filament was used for the measurements that exerts an increasing upward force at a constant rate (6.25 g/s) with a maximum cut-off force of 50 g. The filament was placed under the plantar surface of the hind paw. Measurement was stopped when the paw was withdrawn, and the results were expressed as paw withdrawal thresholds in grams. The pain thresholds were registered before the i.t. drug injections (baseline at 0 min) and then in every 15 min for 90 min. The parent drugs (oxycodone (20 μg), JWH-018 (20 μg), Tyr-D-Ala-Gly-Phe-NH$_2$ (7 μg)) and the bivalent compounds **11** (20 μg) and **19** (20 μg) were injected over 120 s in a volume of 10 μL, followed by 8 μL flush of physiological saline within 60 s. The control animals were injected with the vehicle of the compounds

(physiological saline containing 5% DMSO). The i.t. drug effect was analysed on the MIA-injected hind paws, since none of the treatments influenced the pain threshold at the contralateral side.

Paw withdrawal thresholds on the inflamed side were transformed to % maximum possible effect (%MPE) by the following formula: %MPE = [(observed threshold − baseline threshold)/(50 − baseline threshold)] × 100. It was calculated for the early (15–45 min) and late phase (60–90 min) after drug administration. Therefore, 100% MPE means perfect relief of allodynia (equivalent to a cut-off value of 50 g for all measurements), while 0% MPE means that the observed threshold is equivalent to the baseline value.

2.38. Data analysis

The direct saturation isotherms were determined to obtain the equilibrium dissociation constant (K_d) and the receptor density (B_{max}). In competition binding studies, the inhibitory constants (K_i) were calculated from the inflexion points of the displacement curves using nonlinear least-square curve fitting option and the Cheng-Prusoff equation as $K_i = EC_{50}/(1 + [ligand]/K_d)$. In [^{35}S] GTPγS binding studies, data were expressed as the percentage stimulation of the specific [^{35}S]GTPγS binding over the basal activity. Each experiment was performed in triplicate and analysed with the sigmoid dose-response curve fitting option to obtain potency (ED_{50}) and efficacy (E_{max}). Statistical comparison of E_{max} and EC_{50} values were performed by one-way ANOVA followed by the Bonferroni's multiple comparison test (***$P < 0.001$; **$P < 0.01$); E_{max} values of **11** and **19** in the presence of 10 μM naloxone were compared to the basal activity by unpaired Student's t-test, #$P < 0.05$).

The time-course data sets of the hot plate test and the von Frey tests were examined by two-way ANOVA. The significance of differences between the experimental and control groups was calculated by using the Fisher LSD test for *post hoc* comparison ($P < 0.05$ was considered significant). All data and curves were analysed by the GraphPad Prism 5.0 Software, San Diego, CA, USA.

3. Results and discussion

The bivalent compounds were prepared in a convergent way. The MOR and CB agonists were conjugated via short spacers of different length (4–15 atoms) and polarity (Scheme 1). Oxycodone and JWH-018 were modified at the 6-oxo and at the N-pentyl groups, respectively, to obtain the key intermediates. In the case of the peptidic compounds the C-terminal carboxyl function of the peptide acids was used for the conjugation. Condensation of oxycodone with 2-(aminooxy)acetic acid in EtOH resulted in the linker conjugated O-carboxymethyl ketoxime **1**. Due to the α-effect the ketoximes are stable at physiological pH [48,49], therefore the bivalent ligands are probably stable against hydrolysis. Then the carboxymethyl group of **1** was activated as an O-benztriazolyl ester that was used for the N-acylation of the mono-protected diamine spacers N-Boc-ethylenediamine, N-Boc-1,6-diaminohexane and N-Boc-4,7,10-trioxa-1,13-tridecanediamine. The final acidolytic removal of the Boc protecting group resulted in the amines **5**–**7**.

JWH-018 was functionalized by introducing a terminal carboxyl group to the N-pentyl substituent of the indole ring (Scheme 1). This modification does not affect the aromatic groups of JWH-018 that are responsible for aromatic interactions with the CB receptors [50]. Furthermore, the introduction of heteroatoms to the alkyl group may be tolerated by CB_1 receptors as in the case of the morpholino group of WIN-55,212−2 [51,52]. The carboxyl derivative of JWH-018 (**9**) was prepared in a way analogous to that reported by Huffman et al. [50] The N-alkylation of indole was

achieved with 6-bromohexanoic acid, then **8** was selectively acylated at position 3 with 1-naphthoyl chloride in the presence of Et_2AlCl. Finally, **9** was activated as an O-benztriazolyl ester and it was used for the N-acylation of the amines **5**–**7** resulting in the bivalent compounds **10**–**12**.

The peptidic compounds **18**–**21** were prepared also in a convergent way (Scheme 2). Glycine, 3-aminopropanoic acid or 4-aminobutanoic acid were used as spacers between the opioid and cannabinoid pharmacophores. Indole was regioselectively acylated with 1-naphthoyl chloride and the resulting 3-(α-naphthoyl)-indole (**13**) was N-alkylated with N-Boc-5-bromopentane-1-amine (**14**). Acidolytic deprotection of the carbamate **15** resulted in the JWH-018 derivative **16** with a terminal amine in the N-pentyl group. The N-acetylation of **16** with Ac_2O resulted in the control compound **17**. The elongation of **16** with the opioid peptide or with a spacer amino acid followed by the opioid peptide were achieved in stepwise Boc/tBu solution phase peptide synthesis using EDC and HOBt as coupling agents.

### 3.1. Preparation and validation of [^{3}H]JWH-018

The in vitro characterization of the bivalent compounds in radioligand displacement studies required appropriate opioid and cannabinoid radioligands. The most commonly used CB radioligands in heterologous competition binding experiments are [^{3}H] CP-55,940, [^{3}H]HU-243, [^{3}H]WIN-55,212−2, [^{3}H]SR-141716A (rimonabant), [^{3}H]SR-144528 and [^{3}H]Sch225336 [53]. The structural diversity of the CB receptor ligands [54] and the presence of allosteric site on the CB receptors [55] prompted us to prepare a novel radioligand relevant for the investigation of the CB receptor binding affinities of the JWH-018 containing bivalent compounds. JWH-018 was labeled with tritium as outlined in Scheme 3 and the resulting radioligand was validated in vitro. N-Alkylation of 5-bromoindole with 1-iodopentane was achieved in the presence of triethylamine followed by acylation with 1-naphthoyl chloride that resulted in the brominated precursor **25**. Then **25** was dehalogenated with tritium gas under heterogeneous catalytic conditions and [^{3}H]JWH-018 (**26**) was obtained with a specific activity of 1.48 TBq/mmol. In a similar way, JWH-018 (**24**) was also prepared for the radioligand binding experiments.

Before its application in radioligand competition assays, [^{3}H] JWH-018 was characterized in various in vitro receptor binding experiments. Association and dissociation binding experiments were performed to characterize the interaction of [^{3}H]JWH-018 with membrane receptors using rat brain membrane homogenate that contains both CB_1 and CB_2 receptors [56–59]. Association binding experiments were carried out in the presence of 0.6 nM [^{3}H]JWH-018 at 30 °C and they revealed specific binding of [^{3}H] JWH-018 to rat brain membranes (Fig. 1A). At this temperature the specific binding determined in the presence of 10 μM **24** reached steady-state after 40 min, and it remained stable up to 90 min, the longest incubation time investigated (not shown). The specific binding was found to be 65% of the total binding at 0.6 nM radioligand concentration under equilibrium conditions. Analyzing the association curve provided an observed pseudo-first order rate constant (k_{obs}) of 0.124 ± 0.01 min^{-1}. In the dissociation experiments, rat brain membranes were incubated with 0.6 nM of [^{3}H] JWH-018 at 30 °C for 60 min and dissociation of the ligand−receptor complex was initiated by the addition of 10 μM **24** at different incubation periods (Fig. 1B). It was found that 60% of the radioligand dissociated from the membranes. Dissociation proceeded with a monophasic kinetics and it resulted in a dissociation rate constant (k_d) of 0.105 ± 0.01 min^{-1}. The equilibrium dissociation constant (K_d) calculated from the kinetic data was 3.4 nM under our experimental conditions. Saturation binding
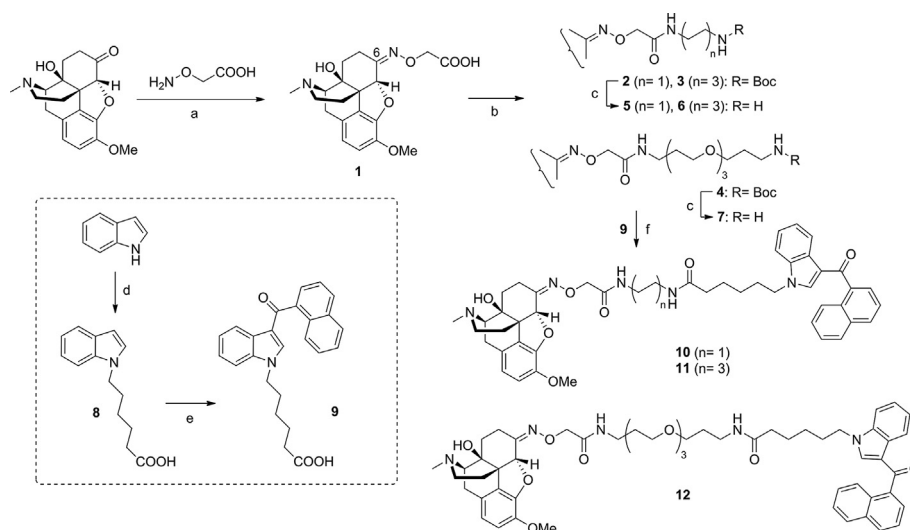
Scheme 1. Preparation of oxycodone − JWH-018 bivalent compounds.
Reagents and conditions: a) EtOH, pyridine, 80 °C, 75 min, 93%; b) HOBt, DIC, DIEA, DMF, 50 °C, 16 h, 81% (**2**), 77% (**3**), 66% (**4**); c) TFA/DCM (1:1), rt, 30 min, 95% (**5**), 96% (**6**), 95% (**7**); d) 6-bromohexanoic acid, TEA, ACN, 80 °C, 16 h, 77% (**8**); e) 1-naphthoyl chloride, Et$_2$AlCl, DCM, 0 °C, 16 h, 42% (**9**); f) HOBt, DIC, DIEA, DMF, 50 °C, 16 h, 79% (**10**), 71% (**11**), 61% (**12**).
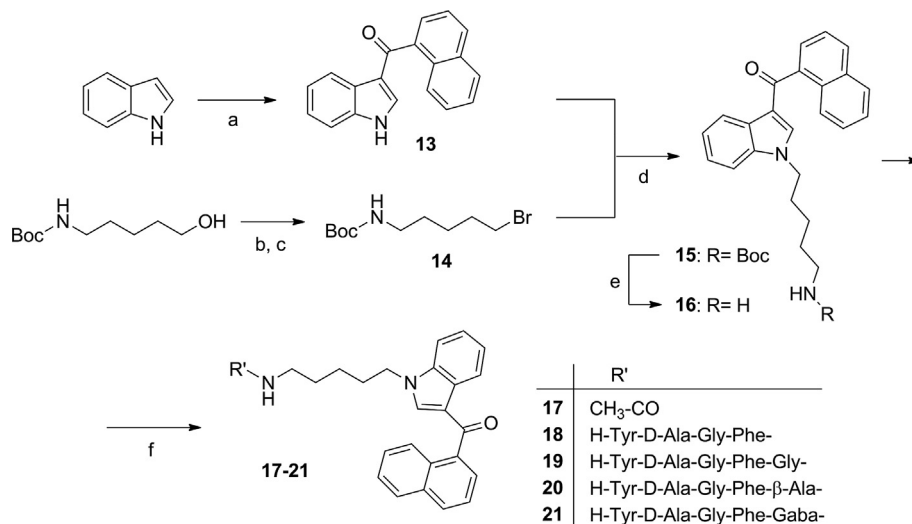
Scheme 2. Preparation of peptide − JWH-018 bivalent compounds.
Reagents and conditions: a) 1-Naphthoyl chloride, Et$_2$AlCl, DCM, 0 °C, 16 h, 70%; b) MsCl, TEA, DCM, −10 °C, 5 h; c) LiBr, THF, reflux, 16 h, 72% (**14**); d) NaH, DMF, 80 °C, 18 h, 85%; e) TFA/DCM (1:1), rt, 30 min, 97%; f) Ac$_2$O, TEA, DCM, rt, 16 h, 91% (**17**), or Boc stepwise peptide synthesis: EDC, HOBt.H$_2$O, NMM, DMF, DCM, and deprotection with TFA/DCM (1:1), rt, 30 min; overall yields 21% (**18**), 14% (**19**), 25% (**20**), 12% (**21**).
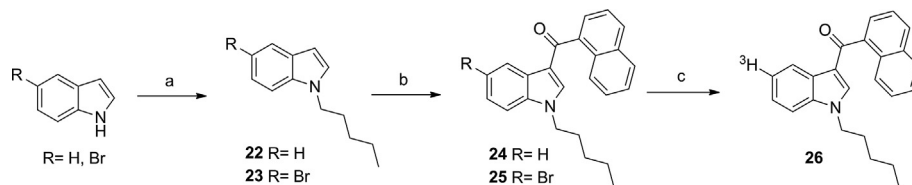
Scheme 3. Tritium labeling of JWH-018.
Reagent and conditions: a) (**22**) 1-iodopentane, TEA, ACN, 80 °C, 16 h, 75%, (**23**) 1-iodopentane, NaOH, DMF, rt, 4 h, 66%; b) Et$_2$AlCl, 1-naphthoyl chloride, DCM, 0 °C, 16 h, 72% (**24**), 82% (**25**); c) ^{3}H$_{2(g)}$, Pd/C, EtOAc, TEA, rt, 4 h.

experiments were then performed to determine the K_d and B_{max} values. The radioligand was incubated with rat brain membranes at increasing concentrations (0−35 nM) in the absence or presence of **24**. The specific binding of [^{3}H]JWH-018 was found to be saturable

and of high affinity in the nanomolar range (Fig. 1C). A single-site binding was calculated from the non-linear fitting of the specific binding data and resulted in an apparent K_d value of 6.5 ± 1.22 nM and a high receptor density (B_{max}) of 1120 ± 89 fmol/mg protein.
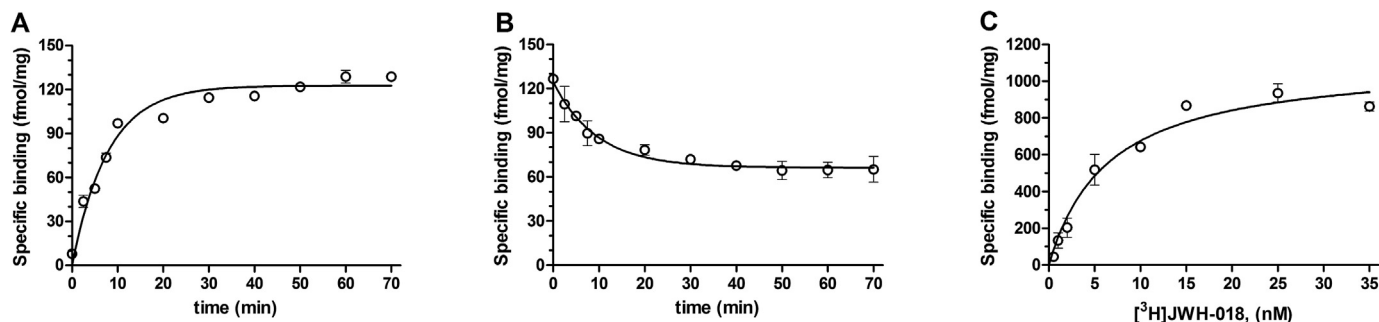
Fig. 1. Binding of [3H]JWH-018 to rat whole brain membrane homogenates (0.45 mg/mL protein). (A) Association and (B) dissociation time courses of [3H]JWH-018 at 30 °C; (C) saturation isotherm of specific CB receptor binding of [3H]JWH-018 at 30 °C for 60 min incubation. Data are means ± SEM (n ≥ 3).

Because [3H]JWH-018 labeled membrane receptors of the rat brain membrane homogenate with high densities and it displayed specific binding to a receptor protein, the binding site of [3H]JWH-018 was further investigated in competition experiments using selective and non-selective cannabinoid ligands. The displacement curves are summarized in Fig. 2 and the calculated inhibitory constants (K_i) are summarized in the table of Fig. 2. In homologous displacement experiments the full agonist JWH-018 exhibited a K_i value of 3.4 ± 0.80 nM. WIN-55,212−2, another full cannabinoid ligand displayed high affinity to the JWH-018 binding sites, while the partial agonist Δ^9-THC competed for the JWH-018 binding sites with 11-times lower affinity. The CB2 receptor selective, inverse agonist AM 630 was found to be effective in displacing [3H] JWH-018 from CB2 receptors. Further experiments revealed that the CB1 receptor selective antagonist/inverse agonist rimonabant and the structurally very similar CB1 selective antagonist/inverse

agonist AM 251 were less effective in displacing [3H]JWH-018 from CB1 receptors on rat brain membrane homogenate. AM 251 displaced 80% of the radioligand from JWH-018 binding sites, while the CB2 selective inverse agonist AM 630 displaced approximately 70% of [3H]JWH-018 from CB2 receptors on rat brain membrane homogenate. Compound **25** was also investigated in heterologous displacement studies, because beside to be a precursor for tritium labeling it is a potentially bioactive JWH-018 derivative substituted at position 5 with bromine. It exhibited good CB receptor affinity in displacing [3H]JWH-018 with a K_i value of 59 ± 3.3 nM. Interestingly, the 5-bromo-substituted intermediate **25** exhibited receptor affinity similar to that of rimonabant, AM 630 and AM 251. Furthermore, the results show that JWH-018 is a non-selective full agonist in the low nanomolar range with a CB1/CB2 receptor selectivity ratio of 3 (K_i(AM 251) = 69 ± 9.1 nM)/K_i(AM 630) = 23 ± 19 nM) that is similar to other reported data [39]. In our
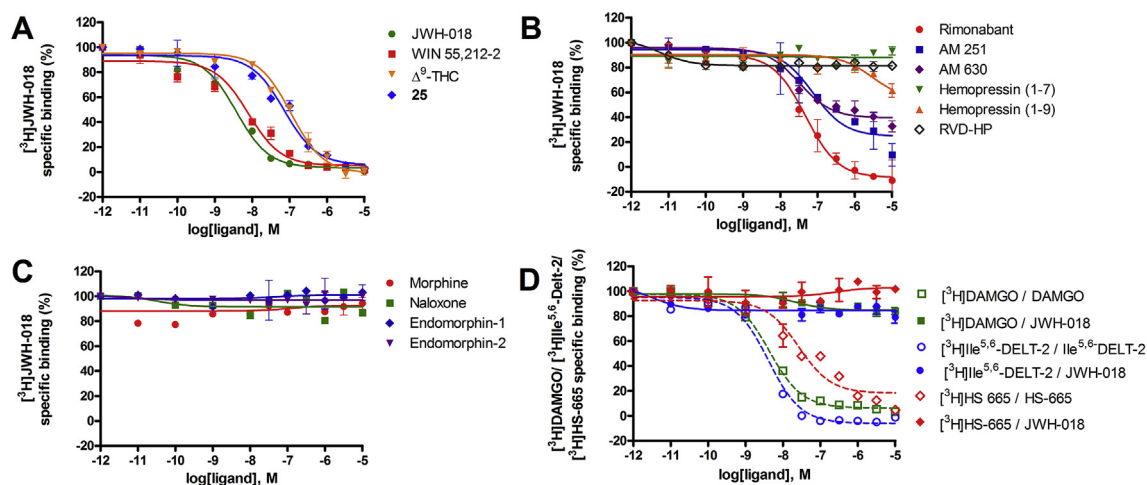
Cannabinoid ligands	K_i (nM)	Cannabinoid ligands	K_i (nM)
JWH-018 (**24**)	3.4 ± 0.8	AM 251	69 ± 9.1
WIN-55,212-2	7.2 ± 2.8	AM 630	27 ± 2.2
Δ^9-THC	82 ± 4.5	Hemopressin (1-7)	>10000
25	59 ± 3.3	Hemopressin (1-9)	2793 ± 41
Rimonabant	43 ± 5.5	RVD-Hemopressin	>10000

Fig. 2. Characterization of JWH-018 binding sites in competition binding experiments in rat or guinea pig ([3H]HS-665) whole brain membrane homogenates. (A–C) The specific binding of [3H]JWH-018 in the presence of unlabeled cannabinoid or opioid ligands. (D) The specific binding of the MOR, DOR and KOR specific radioligands [3H]DAMGO, [3H]Ile5,6-deltorphin-2 and [3H]HS-665, respectively, in the presence of JWH-018 (filled symbols) or in the presence of the corresponding unlabeled opioid ligand (open symbols). Data are mean percentage of specific binding ± SEM (n ≥ 3). Table shows the calculated inhibitory constants against [3H]JWH-018. K_i values were as $K_i = EC_{50}/(1 + [ligand]/K_d)$, where $K_d = 6.5$ nM was obtained from the saturation experiment, data are means ± SEM, n ≥ 3.

experimental model, the investigated cannabinoid ligands competed for [³H]JWH-018 binding sites with the following order of potency: JWH-018 > WIN-55,212−2 > AM 630 > rimonabant > **25** > AM 251 > Δ^9-THC > hemopressin(1−9).

Next, competition binding experiments were performed to compare the ability of the endogenous peptide cannabinoid RVD-hemopressin and its derivatives hemopressins(1−7) and (1−9) to inhibit the binding of [³H]JWH-018 in rat brain membrane homogenate. It was found that neither the *N*- and *C*-terminally truncated hemopressin(1−7) [60], nor the CB₁ negative and CB₂ receptor positive allosteric modulator, RVD-hemopressin [61,62] could displace the bound radioligand. Only the nonapeptid CB₁ inverse agonist/antagonist hemopressin(1-9) [63] was able to compete with [³H]JWH-018, with an apparently high inhibitory constant of 2793 ± 4.1 nM, however, hemopressin(1−9) only partially (c.a. 40%) displaced [³H]JWH-018. These results indicated that the allosteric binding site of the peptidic ligands is different from that of the non-peptidic cannabinoid agonists/inverse agonists, and that JWH-018 probably bound to the CB receptors at the orthosteric binding site.

It was also important to investigate whether [³H]JWH-018 interacts with the opioid receptors because this radioligand was prepared to characterize the CB receptor binding of the opioid − cannabinoid bivalent ligands. The effects of the opioid ligands morphine, naloxone and endomorphins-1 and -2 on the specific binding of [³H]JWH-018 were measured in the presence of increasing concentration of the opioids. It was found that none of them decreased the specific binding of [³H]JWH-018 even at a concentration of 10 μM, meaning that [³H]JWH-018 did not bind to the opioid receptors (Fig. 2C). Finally, competition binding experiments were carried out to evaluate the ability of JWH-018 to inhibit specific binding of the μ-, δ- and κ-opioid receptor (MOR, DOR and KOR) selective radioligands [³H]DAMGO, [³H]Ile⁵,⁶-deltorphin-2 and [³H]HS-665 [64], respectively (Fig. 2D). For KOR binding the guinea pig brain was used because it contains KORs in higher density than the rat brain. It was found that JWH-018 did not exhibited any binding affinity to the MOR, DOR and KOR when compared to the homologue displacements with DAMGO, Ile⁵,⁶-deltorphin-2 or HS-665, respectively.

3.2. Receptor binding properties of the synthetic compounds

In order to assess the effects of the structural changes of the monomeric ligands on the biological activity, and to evaluate the bivalent compounds for affinity and selectivity, the novel synthetic compounds were subjected to radioligand binding assays. Displacements of the MOR selective radioligand [³H]DAMGO, the DOR selective [³H]Ile⁵,⁶-deltorphin-2, the KOR selective [³H]HS-665 and the cannabinoid radioligands [³H]JWH-018 and [³H]WIN-55,212-2 by the synthetic compounds were investigated in rat or guinea pig brain membrane homogenates. It was found that the modification of oxycodone at position 6 with *O*-carboxymethyl oxime (**1**) resulted in a 2.7-fold loss of MOR affinity, a 4-fold increased affinity for the DOR and loss of KOR affinity (Figure S1, Table 1). The MOR selectivity of oxycodone over DOR was reduced by the introduction of the linker group in **1** as the $K_{i\delta}/K_{i\mu}$ ratio decreased from 55 to 5. The introduction of a terminal carboxyl function to the pentyl chain of JWH-018 (**9**) decreased the CB receptor affinity 70-fold. The introduction of the ethylenediamine (**5**) and the 1,6-diaminohexane spacers (**6**) resulted in 2-fold and 5-fold loss of MOR affinity, respectively, while the incorporation of the *O*-,*O*′-bis(3-aminopropyl)-diethyleneglycol spacer (**7**) resulted in an 8-fold loss of MOR affinity as compared to the parent compound oxycodone. The bivalent compounds **10**−**12** exhibited good affinity to the MOR that was only 2−4-fold lower than the MOR affinity of

oxycodone. The selectivity of **10**−**12** for the MOR over DOR was 15−19, while their MOR selectivity over KOR was found to be 9−10. In competition binding experiments the capabilities of the bivalent compounds **10**−**12** to displace [³H]JWH-018 and [³H]WIN-55,212−2 were investigated, and it was found that they displaced 40−70% of the specific bound radioligands [³H]JWH-018 or [³H]WIN-55,212−2. The bivalent compound **10** exhibited the highest CB receptor affinity against [³H]WIN-55,212−2, however **11** displaced [³H]JWH-018 most efficiently.

Next, the peptidic compounds were evaluated for affinity and selectivity by radioligand displacement assays (Figure S2, Table 2). The opioid pharmacophore Tyr-D-Ala-Gly-Phe-NH₂ exhibited high affinity to the MOR ($K_i = 0.8$ nM), 130-times weaker affinity to the DOR and 210-times weaker affinity to the KOR, and it had no affinity to the CB receptors. The introduction of a terminal amino group into the pentyl chain of JWH-018 (**16**) led to decreased affinity to the [³H]JWH-018 or [³H]WIN-55,212-2 labeled binding sites. However, *N*-acetylation of **16** diminished the positively charged functional group and the CB receptor affinity of **17** was found to be higher ($K_i = 145$ nM) than that of **16**. When **16** was *N*-acylated with Tyr-D-Ala-Gly-Phe-OH or with its *C*-terminally extended derivatives, the resulting bivalent compounds **18**−**21** exhibited moderate change in MOR, DOR and KOR affinity. The binding affinity of **19** and **21** for KOR was 2−3 times higher than that of the Tyr-D-Ala-Gly-Phe-NH₂. In [³H]JWH-018 and [³H]WIN-55,212-2 displacement experiments **19** exhibited the highest affinity to the CB receptors among the peptidic bivalent compounds ($K_i = 251$ and 317 nM, respectively), and **19** was able to decrease the [³H]JWH-018 and [³H]WIN-55,212-2 specific binding by about 45−50%. In contrast, the CB receptor affinity of **18**, **20** and **21** decreased significantly.

In the next step the signaling properties of the bivalent compounds were investigated in ligand stimulated [³⁵S]GTPγS binding experiments in rat brain membrane homogenate (Figure S3, Tables 1 and 2). This tissue preparation abundantly contains both MOR and CB receptors, therefore it is an appropriate model to investigate the [³⁵S]GTPγS binding stimulation capability of the MOR and CB agonists and their derivatives [65,66]. The oxime **1** exhibited lower potency than oxycodone, and significant reduction of the stimulatory effect was observed. Coupling of the spacers to **1** decreased the efficacy, and the partial opioid agonist oxycodone became weaker partial agonists/neutral antagonists. The tetrapeptide H-Tyr-D-Ala-Gly-Phe-NH₂ increased the G-protein basal activity with a maximum efficacy of 157% and with a potency of 191 nM. The full agonist JWH-018 efficiently stimulated the G-proteins, demonstrated low potency (69 nM) and high stimulatory activity (163%). The introduction of the carboxyl function in **9** changed the full agonist to a weak inverse agonist. The amine **16** acted as an antagonist on CB receptors, since it did not stimulate G-proteins but displayed a considerable CB receptor affinity. The *N*-acetylated compound **17** reduced [³⁵S]GTPγS specific binding significantly by nearly 20% as compared to the basal activity level, indicating an inverse agonistic effect. The weak inverse agonistic effect of **17** might be mediated through CB receptors, since it showed a relatively good affinity to the [³H]JWH-018 binding site. The bivalent compounds **10** and **12** did not induce significant changes in basal [³⁵S]GTPγS binding, however these compounds displayed noticeable MOR and CB receptor affinity. In contrast, **11** exhibited high G-protein stimulatory effect ($E_{max} = 147 \pm 3.8\%$, $EC_{50} = 215 \pm 4.5$ nM) demonstrating the agonist character of **11**.

To explore the activation of MOR and/or CB₁/CB₂ receptor-mediated signaling induced by **11**, the G-protein activation was investigated in the absence or presence of 10 μM naloxone, 10 μM rimonabant or 10 μM AM 630 in rat brain membrane homogenate (Fig. 3). The stimulatory effect of 10 μM **11** ($E_{max} = 147 \pm 4.0\%$,

Table 1
Inhibitory constant values and signaling properties of oxycodone and JWH-018 derivatives.

compd.	K_i (nM)							E_{max} (%)	EC_{50} (nM)
	[³H]DAMGO	[³H]Ile⁵,⁶-deltorphin-2	[³H]HS-665	$K_{i\delta}/K_{i\mu}$	$K_{i\kappa}/K_{i\mu}$	[³H]JWH-018	[³H]WIN-55,212-2		
oxycodone	8.9 ± 0.4	487 ± 36	325 ± 32	55	37	>10000	>10000	135 ± 4.6	51 ± 2.5
JWH-018	>10000	>10000	>10000	–	–	3.4 ± 0.8	2.9 ± 0.4	163 ± 3.1	69 ± 10
1	24 ± 0.2	110 ± 14	>10000	5	–	n.d.	n.d.	109 ± 3.2	225 ± 27
5	17 ± 0.9	533 ± 33	471 ± 44	31	28	n.d.	n.d.	113 ± 2.1	450 ± 11
6	41 ± 3.6	659 ± 14	380 ± 43	16	10	n.d.	n.d.	111 ± 2.5	305 ± 14
7	74 ± 3.0	757 ± 55	503 ± 50	10	7	n.d.	n.d.	112 ± 7.1	200 ± 55
9	n.d.	n.d.	n.d.	–	–	247 ± 48	205 ± 28	81 ± 4.7	4225 ± 148
10	33 ± 4.0	623 ± 43	337 ± 40	19	10	255 ± 47	9.3 ± 1.8	100 ± 1.7	n.r.
11	18 ± 5.0	263 ± 15	172 ± 19	15	10	34 ± 8	12 ± 3.5	147 ± 3.8	215 ± 4.5
12	20 ± 1.0	386 ± 23	186 ± 37	19	9	183 ± 32	78 ± 23	99 ± 1.2	n.r.

K_i values were obtained from the displacement curves shown in Figure S1, n.d. not determined; The E_{max} and EC_{50} values were calculated from the dose-response curves of Figure S3, n.r.: not relevant. Data are means ± SEM, n ≥ 3.

Table 2
Inhibitory constant values and signaling properties of peptidic compounds.

compd.	K_i (nM)							E_{max} (%)	EC_{50} (nM)
	[³H]DAMGO	[³H]Ile⁵,⁶-deltorphin-2	[³H]HS-665	$K_{i\delta}/K_{i\mu}$	$K_{i\kappa}/K_{i\mu}$	[³H]JWH-018	[³H]WIN-55,212-2		
Tyr-D-Ala-Gly-Phe-NH₂	0.8 ± 0.1	107 ± 19	173 ± 15	134	216	>10000	>10000	157 ± 3.9	191 ± 7
JWH-018	>10000	>10000	>10000	–	–	3.4 ± 0.8	2.9 ± 0.4	163 ± 3.1	69 ± 10
16	n.d.	n.d.	n.d.	–	–	190 ± 17	269 ± 21	102 ± 3.5	n.r.
17	n.d.	n.d.	n.d.	–	–	145 ± 13	149 ± 18	83 ± 5.6	2154 ± 100
18	50 ± 2.7	214 ± 2.0	231 ± 45	4	5	1013 ± 45	823 ± 62	110 ± 3.8	1801 ± 102
19	2.1 ± 0.3	134 ± 12	63 ± 13	64	30	251 ± 18	317 ± 47	160 ± 1.9	114 ± 10
20	48 ± 5.1	190 ± 33	151 ± 25	4	3	919 ± 48	1216 ± 102	114 ± 1.6	18 ± 6
21	20 ± 3.5	92 ± 25	50 ± 15	5	3	928 ± 45	1042 ± 28	125 ± 1.5	60 ± 10

K_i values were obtained from the displacement curves shown in Figure S2, n.d. not determined; The E_{max} and EC_{50} values were calculated from the dose-response curves of Figure S3, n.r.: not relevant. Data are means ± SEM, n ≥ 3.

$EC_{50} = 224 ± 5.0$ nM) was reduced by the opioid antagonist naloxone [67] (10 μM) ($E_{max} = 112 ± 2.1$%, $EC_{50} = 397 ± 34$ nM). But naloxone did not reduce the G-protein stimulatory effect to the basal level, and the residual activity suggested that **11** could activate the CB receptors as well. The CB₁ antagonist/inverse agonist rimonabant (10 μM) slightly antagonized the G-protein stimulatory
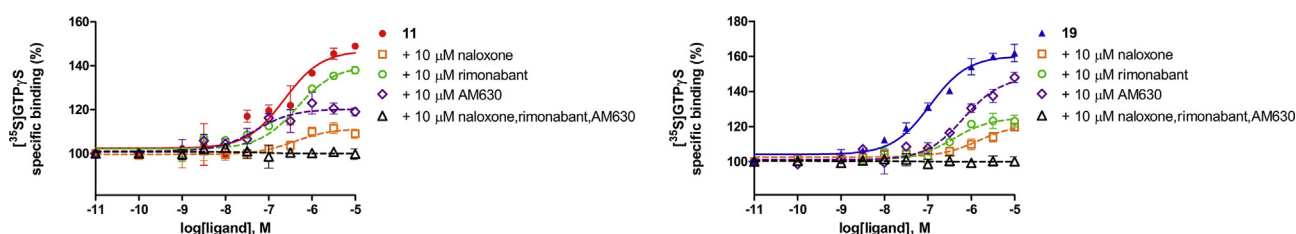
	E_{max} (%)	EC_{50} (nM)
11	147 ± 4.0	224 ± 5.0
11 + 10 μM naloxone	112 ± 2.1[***/#]	397 ± 34[***]
11 + 10 μM rimonabant	139 ± 2.4[***]	452 ± 24[***]
11 + 10 μM AM 630	122 ± 2.7[***]	340 ± 7.5[***]
11 + 10-10 μM (naloxone, rimonabant, AM 630)	100 ± 1.1[***]	n.r.
19	160 ± 1.9	112 ± 7.5
19 + 10 μM naloxone	121 ± 2.5[***/#]	1473 ± 118[***]
19 + 10 μM rimonabant	125 ± 1.9[***]	378 ± 20[***]
19 + 10 μM AM 630	148 ± 3.0[***]	671 ± 12[***]
19 + 10 μM (naloxone, rimonabant, AM 630)	100 ± 1.2[***]	n.r.

Fig. 3. Opioid and cannabinoid receptor-mediated effects of **11** and **19** on G-protein activation in [³⁵S]GTPγS binding assays in rat brain membrane homogenates. Figures represent relative specific binding of [³⁵S]GTPγS with the increasing concentrations (10⁻¹⁰–10⁻⁵ M) of **11** or **19** in the absence or presence of 10 μM naloxone, 10 μM rimonabant or 10 μM AM 630. Data are mean percentage of specific binding ± SEM (n = 3–5) over the basal activity. The calculated maximal G-protein stimulation efficacy (E_{max}) and ligand potency (EC_{50}) values are listed. Statistical comparison of E_{max} and EC_{50} were performed by one-way ANOVA followed by the Bonferroni's multiple comparison test (***, $P < 0.001$). # indicates significant difference (unpaired Student's t-test, $P < 0.05$) in the E_{max} of **11** or **19** in the presence of 10 μM naloxone compared to the basal activity. n.r. not relevant.

effect of **11** ($E_{max} = 139 \pm 2.4\%$, $EC_{50} = 452 \pm 24$ nM), while the CB_2 antagonist/inverse agonist AM 630 (10 µM) had greater antagonistic effect ($E_{max} = 122 \pm 2.7\%$, $EC_{50} = 340 \pm 7.5$ nM). In order to decrease the stimulatory effect of **11** to the basal level, the copresence of naloxone, rimonabant and AM 630 was required.

The peptidic bivalent compounds **18**, **20** and **21** exhibited significantly decreased capability of G-protein activation, but **19** exhibited signaling with a maximum efficacy of 160% that was similar to that of the parent opioid and cannabinoid compounds. The binding affinity of **19** to the opioid receptors remained nearly the same as the parent tetrapeptide amide or **24**. The stimulatory effect of 10 µM **19** ($E_{max} = 160 \pm 1.9\%$, $EC_{50} = 112 \pm 7.5$ nM) was partially reduced by the opioid antagonist naloxone [67] ($E_{max} = 121 \pm 2.5\%$, $EC_{50} = 1473 \pm 118$ nM), and the residual activity of **19** indicated CB receptor activation (Fig. 3). In contrast to **11**, the CB_2 antagonist/inverse agonist.

AM 630 exerted weak antagonistic effect to **19** ($E_{max} = 148 \pm 3.0\%$, $EC_{50} = 671 \pm 12$ nM), however, the CB_1 antagonist/inverse agonist rimonabant could antagonize more efficiently the G-protein activation effect of **19** ($E_{max} = 125 \pm 1.9\%$, $EC_{50} = 378 \pm 20$ nM). The stimulatory effect of **19** decreased to the basal level in the copresence of naloxone, rimonabant and AM 630. Taken together, these interactions indicated both an opioid and a CB receptor dependent agonist effect of **11** and **19**.

Because the bivalent compounds **10** and **12** with noticeable MOR and CB receptor affinity did not induce significant changes in basal [^{35}S]GTPγS binding, their antagonist effect was investigated in details. In control experiments the G-protein stimulatory agonist effect of oxycodone was antagonized by the opioid antagonist naloxone, and that of JWH-018 was antagonized by the co-addition of the CB_1 selective rimonabant and the CB_2 selective AM 630. It was found that the maximum agonist effects of oxycodone, Tyr-D-Ala-Gly-Phe-NH$_2$, JWH-018, **11** and **19** were reduced to the basal level by compounds **10** and **12** as well (Fig. 4). These data demonstrated that compounds **10** and **12** acted as antagonists of the MOR and CB receptors.

3.3. Permeability of 11 and 19 through the brain endothelium

In order to evaluate whether the agonist bivalent compounds **11** and **19** can effectively target central or peripheral opioid and CB receptors, the permeability of [^{3}H]**11** and [^{3}H]**19** through brain endothelial cells was measured using a well characterized triple co-culture blood-brain barrier (BBB) model [45,46]. The required tritium labeled bivalent compounds were prepared from iodinated precursor compounds. Compound **9** was iodinated with iodine monochloride in MeOH then it was reduced with tritium gas. The amine **6** was then N-acylated with [^{3}H]**9** under the conditions outlined in Scheme 1 that yielded [^{3}H]**11**. In the case of **19**, bis(-pyridine)iodonium(I) tetrafluoroborate [68] was used to prepare the iodo-derivative of **19** that was reduced with tritium gas to obtain [^{3}H]**19**. In the in vitro BBB permeability measurement [^{3}H]**11** and [^{3}H]**19** were applied in 0.25 and 0.75 µM concentrations and their fluxes in the blood to brain direction was measured. Similar endothelial permeability coefficients were calculated ($2-3 \times 10^{-6}$ cm/s) for both molecules at both donor concentrations (Fig. 5). This value is not significantly different from the permeability coefficient of fluorescein, a hydrophilic reference molecule with a limited permeability to the brain. The penetration of **11** and **19** was fifteen times higher across empty inserts indicating that the membrane of the inserts was permeable for the molecules. These experiments indicated the limited penetration of the bivalent compounds **11** and **19** via the BBB, thus, an additional test was

performed using a pain model reflecting supraspinal anti-nociception as the hot plate test.

3.4. Hot plate test

The hot plate test in mice could help to examine whether compounds cross the BBB after peripheral administration and act at the receptors located in the central nervous system. For that compounds **11** and **19** were administered i.v. at a dose of 10 mg/kg, and the effects on the nociceptive threshold were recorded from 15 to 120 min after the injection. The bivalent compounds **11** and **19** slightly increased the thermal latencies after i.v. administration as compared to the vehicle-treated animals, however, the size of the effect was not significant (Fig. 6). These findings confirmed the results of the in vitro study on endothelium permeability, thus, intrathecal administration was applied during in vivo experiments.

3.5. In vivo evaluation of selected bivalent compounds

The antiallodynic effects of **11** and **19** at spinal level were measured in a chronic osteoarthritis pain model and were compared to those of the parent compounds oxycodone, Tyr-D-Ala-Gly-Phe-NH$_2$ and JWH-018. Osteoarthritis was induced by injecting sodium iodoacetate into the tibiodorsal joint of one of the hind legs of rats, and after a 7-day period mechanical allodynia was measured on the inflamed paw in every 15 min for 90 min. It had consistently been shown that sodium iodoacetate caused severe end-stage cartilage destruction resulting in prolonged osteoarthritis-like joint pain which can be treated with classical antinociceptive drugs [69–71]. The percentage maximum possible effect (%MPE) was calculated as the percentage difference between the measured response and the baseline response, divided by the difference between the maximum response and the baseline response [72]. To reveal the duration of the effects of the compounds two phases - the mean values up to 45 min as early phase, and between 60 and 90 min, as the late phase - were analysed. All compounds were applied intrathecally in the same dose (20 µg), except Tyr-D-Ala-Gly-Phe-NH$_2$, that was administered in lower dose (7 µg) because higher dose of the peptide led to rigidity in the animals. The applied doses did not cause visible motor impairments but no detailed behavioral tests were performed to reveal the subtle side effects of these ligands in this respect. These treatments did not influence the mechanosensitivity of the non-inflamed side (mean paw withdrawal force for the baseline, early and late phases: 44 ± 0.8 g, 41 ± 1.2 g and 42 ± 0.9 g, respectively; see supplementary Table S2), therefore, the results were analysed only on the iodoacetate-injected paws. The bivalent compounds **11** and **19**, and all the control compounds had antiallodynic activity during the early phase as they significantly increased the %MPE compared to the vehicle treatment (Fig. 7). Regarding the late phase, the antiallodynic effect of oxycodone declined. The short duration of the oxycodone-induced antinociception was in agreement with the findings of Lemberg et al. [73] However, the bivalent derivatives still produced significant effect, that was similar to the late phase activity of JWH-018. The antiallodynic effects of **11** and **19** were similar to those of oxycodone and JWH-018, and the post hoc analysis did not show any significant differences between the drug-treated groups. However, considering the nmol doses of the applied compounds (the molecular weights of **11** and **19** are ca. twice of the parent ligands; Table S3), Tyr-D-Ala-Gly-Phe-NH$_2$ showed the highest efficacy that was followed by **11** and **19**, and finally by oxycodone, while JWH-018 showed the lowest efficacy. Thus, the possible advantage of **11** and **19** might be that they can
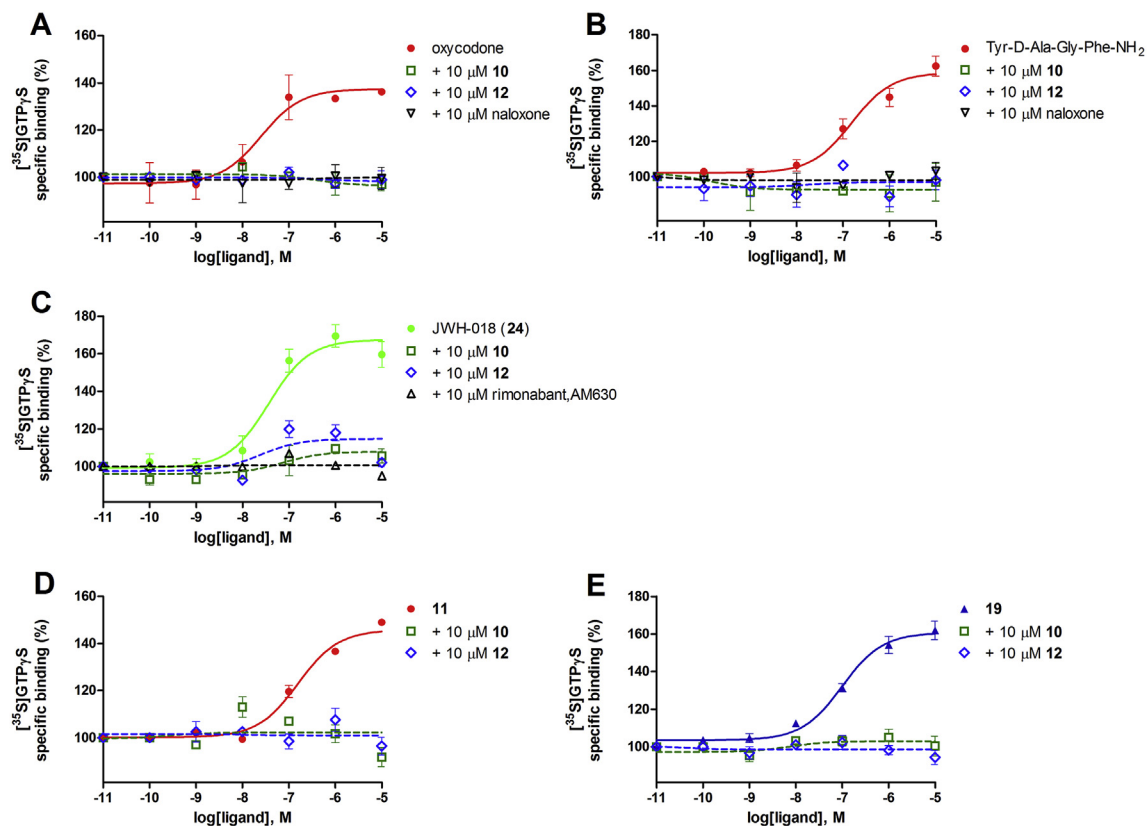
Fig. 4. The antagonist effect of **10** and **12** in agonist induced [^{35}S]GTPγS binding assays in rat brain membrane homogenates. Figures represent relative specific binding of [^{35}S]GTPγS with the increasing concentrations (10^{-10}–10^{-5} M) of oxycodone, Tyr-D-Ala-Gly-Phe-NH$_2$, JWH-018, **11** and **19** in the absence (filled symbols) or in the presence (open symbols) of 10 μM of naloxone, rimonabant, AM 630, **10** or **12**. Data are mean percentage of specific binding ± SEM (n ≥ 3) over the basal activity (100%). The calculated parameters are listed in the Supplementary Table S1.
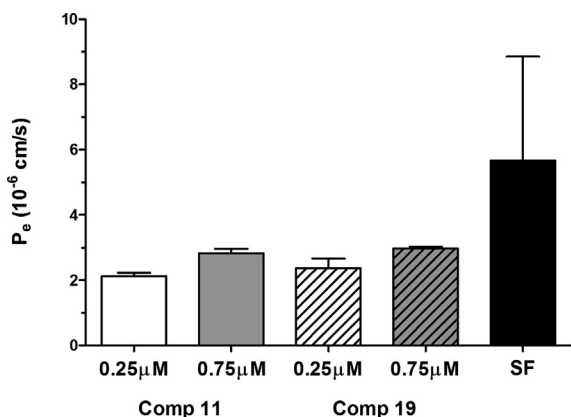
Fig. 5. Evaluation of the flux of compound **11** and **19** across an in vitro BBB model consisting of primary rat brain endothelial cells, pericytes and astrocytes. Permeability of sodium fluorescein (SF) is also given as reference. P_e: permeability coefficient, data are means ± SD, n = 4.

Fig. 6. Time-course effects of i.v. administered bivalent compounds in the hot plate test. Data are means ± SEM, n = 6/group.

reach the same effects as the parent compounds but at lower concentration.

4. Conclusions

The involvement of the MOR and CB receptors in pain management is well documented and numerous studies report the synergistic interaction of the opioid and cannabinoid agonists [3].
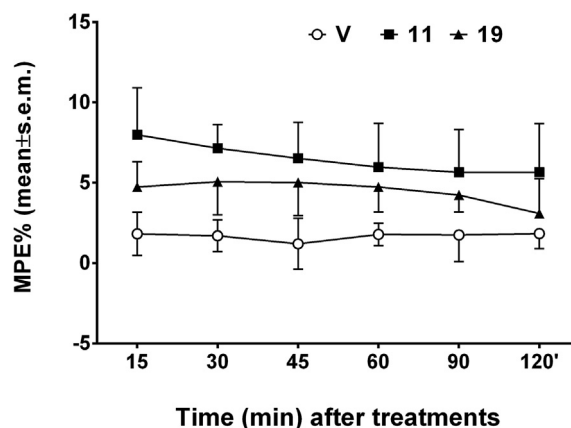
The interaction of the opioid and cannabinoid receptors are hypothesized to undergo at signal transduction level or cannabinoids may trigger the release of endogenous opioid peptides or the endocannabinoid system may be altered by opioids [74]. Direct interaction between the MOR and CB GPCRs may also be a possible molecular mechanisms underlying the interactions of these systems [29]. Multitargeting approaches can be applied to exploit these beneficial interactions, especially in the treatment of chronic pain, because parallel or independent interaction of a bivalent compound, i.e. consisting of two covalently linked
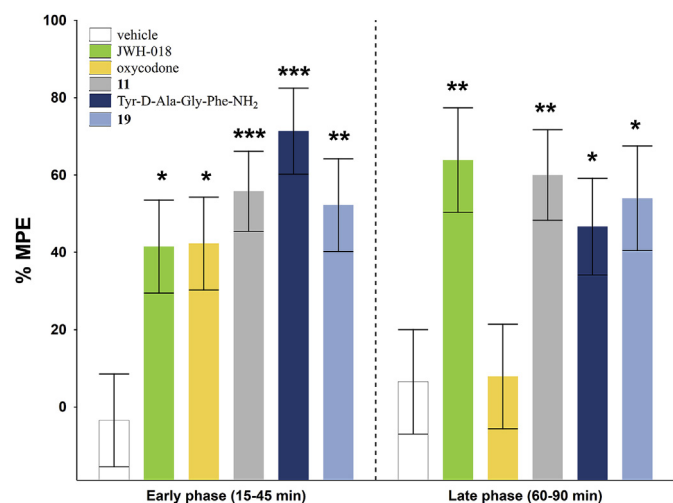
Fig. 7. Time-course effects of i.t. administered selected compounds. Data are means ± SEM, $^{*}P < 0.05$, $^{**}P < 0.01$ and $^{***}P < 0.001$ vs the vehicle-treated group, $n = 6$–8/group.

pharmacophores, with the MOR and CB receptors can be achieved [75]. Furthermore, bivalent compounds may interact with pre-dimerized GPCRs in a cooperative manner that can result in increased affinity of the bivalent ligands relative to the individual binding of the monovalent components. This way the pharmaco-kinetics and pharmacodynamics of the single drugs with substantially different absorption and partition properties will be the same, and a treatment method where the amount of the opioid component is subtherapeutic as compared to the administration without the cannabinoid can be applied.

The strategy of combining GPCR ligands with various spacers to obtain multitargeting ligands is widely investigated with various success [76,77]. In our work JWH-018, a synthetic full agonist of CB receptors was covalently coupled with the semisynthetic opioid agonist oxycodone or with the enkephalin-related tetrapeptide agonist Tyr-D-Ala-Gly-Phe via spacers of different length and hydrophobicity. The structural diversity of the CB receptor ligands [78] and the presence of allosteric sites on the CB receptors prompted us to prepare and validate [^{3}H]JWH-018 as an appropriate radioligand competitor of the bivalent compounds in in vitro experiments. In radioligand binding assays **11** and **19** were found to be able to bind to both the MOR and CB receptors with substantial affinity. These bivalent compounds exhibited agonist-induced G-protein activation with high efficacy, and it was also found that the agonist effects of **11** and **19** were mediated via both the MOR and CB receptors. Compound **11** preferred mainly MOR and CB$_2$, whereas compound **19** preferred MOR and CB$_1$ receptor mediated interactions, that is in agreement with the role of all these receptors in the spinal mechanisms of pain relief [9,66,79–82]. In contrast, **10** and **12** were found to be antagonists at both the MOR and CB receptors and they could antagonize the agonist effects of **11** and **19** in vitro. At spinal level the bivalent compounds **11** and **19** were equieffective with the parent drugs at 20 µg dose in a chronic osteoarthritis pain model in rats. Because MOR and CB receptor agonists can be effectively applied in the treatment of chronic pain including neuropathic pain, these findings can help to develop multitargeting antinociceptive drugs featured with opioid and cannabinoid agonist character in a single molecule.

Author contributions

The manuscript was written through contributions of all authors. All authors have given approval to the final version of the manuscript.

Notes

The authors declare no competing financial interest.

Acknowledgment

Appendix A. Supplementary data

Supplementary data associated with this article can be found in the online version, at https://doi.org/10.1016/j.ejmech.2019.05.037. These data include MOL file and InChiKeys of the most important compounds described in this article.

References

[1] A. Wolkerstorfer, N. Handler, H. Buschmann, New approaches to treating pain, Bioorg. Med. Chem. Lett 26 (4) (2016) 1103–1119.
[2] J. Manzanares, M. Julian, A. Carrascosa, Role of the cannabinoid system in pain control and therapeutic implications for the management of acute and chronic pain episodes, Curr. Neuropharmacol. 4 (3) (2006) 239–257.
[3] S. Nielsen, P. Sabioni, J.M. Trigo, M.A. Ware, B.D. Betz-Stablein, B. Murnion, N. Lintzeris, K.E. Khor, M. Farrell, A. Smith, et al., Opioid-sparing effect of cannabinoids: a systematic review and meta-analysis, Neuropsychopharmacology 42 (9) (2017) 1752–1765.
[4] S.P. Welch, D.L. Stevens, Antinociceptive activity of intrathecally administered cannabinoids alone, and in combination with morphine, in mice, J. Pharmacol. Exp. Ther. 262 (1) (1992) 10–18.
[5] D.L. Cichewicz, Z.L. Martin, F.L. Smith, S.P. Welch, Enhancement of mu opioid antinociception by oral Δ^9-tetrahydrocannabinol: dose-response analysis and receptor identification, J. Pharmacol. Exp. Ther. 289 (1999) 859–867.
[6] D.L. Cichewicz, S.P. Welch, Modulation of oral morphine antinociceptive tolerance and naloxone-precipitated withdrawal signs by oral Δ^9-tetrahydrocannabinol, J. Pharmacol. Exp. Ther. 305 (3) (2003) 812–817.
[7] D.L. Cichewicz, E.A. McCarthy, Antinociceptive synergy between Δ^9-tetrahydrocannabinol and opioids after oral administration, J. Pharmacol. Exp. Ther. 304 (3) (2003) 1010–1015.
[8] S.M. Tham, J.A. Angus, E.M. Tudor, C.E. Wright, Synergistic and additive interactions of the cannabinoid agonist CP55,940 with µ opioid receptor and A2-adrenoceptor agonists in acute pain models in mice, Br. J. Pharmacol. 144 (6) (2005) 875–884.
[9] J. Desroches, J.F. Bouchard, L. Gendron, P. Beaulieu, Involvement of cannabinoid receptors in peripheral and spinal morphine analgesia, Neuroscience 261 (2014) 23–42.
[10] N.P. Kazantzis, S.L. Casey, P.W. Seow, V.A. Mitchell, C.W. Vaughan, Opioid and cannabinoid synergy in a mouse neuropathic pain model, Br. J. Pharmacol. 173 (16) (2016) 2521–2531.
[11] M.B. Yuill, D.E. Hale, J. Guindon, D.J. Morgan, Anti-nociceptive interactions between opioids and a cannabinoid receptor 2 agonist in inflammatory pain, Mol. Pain 13 (2017) 1–15.
[12] D.P. Finn, S.R. Beckett, C.H. Roe, A. Madjd, K.C. Fone, D.A. Kendall, C.A. Marsden, V. Chapman, Effects of coadministration of cannabinoids and morphine on nociceptive behaviour, brain monoamines and HPA axis activity in a rat model of persistent pain, Eur. J. Neurosci. 19 (3) (2004) 678–686.
[13] M.L. Cox, V.L. Haller, S.P. Welch, Synergy between Δ^9-tetrahydrocannabinol and morphine in the arthritic rat, Eur. J. Pharmacol. 567 (1–2) (2007) 125–130.
[14] P.A. Smith, D.E. Selley, L.J. Sim-Selley, S.P. Welch, Low dose combination of morphine and Δ^9-tetrahydrocannabinol circumvents antinociceptive tolerance and apparent desensitization of receptors, Eur. J. Pharmacol. 571 (2–3) (2007) 129–137.

[15] D.R. Maguire, C.P. France, Antinociceptive effects of mixtures of mu opioid receptor agonists and cannabinoid receptor agonists in rats: impact of drug and fixed-dose ratio, Eur. J. Pharmacol. 819 (2018) 217—224.

[16] J.X. Li, L.R. McMahon, L.R. Gerak, G.L. Becker, C.P. France, Interactions between Δ9-tetrahydrocannabinol and mu opioid receptor agonists in rhesus monkeys: discrimination and antinociception, Psychopharmacol. Berl. 199 (2) (2008) 199—208.

[17] D.R. Maguire, W. Yang, C.P. France, Interactions between mu-opioid receptor agonists and cannabinoid receptor agonists in rhesus monkeys: antinociception, drug discrimination, and drug self-administration, J. Pharmacol. Exp. Ther. 345 (3) (2013) 354—362.

[18] D.R. Maguire, C.P. France, Impact of efficacy at the mu-opioid receptor on antinociceptive effects of combinations of mu-opioid receptor agonists and cannabinoid receptor agonists, J. Pharmacol. Exp. Ther. 351 (2) (2014) 383—389.

[19] L.R. Gerak, C.P. France, Combined treatment with morphine and Δ9-tetrahydrocannabinol in rhesus monkeys: antinociceptive tolerance and withdrawal, J. Pharmacol. Exp. Ther. 357 (2) (2016) 357—366.

[20] J.D. Roberts, C. Gennings, M. Shih, Synergistic affective analgesic interaction between Δ9-tetrahydrocannabinol and morphine, Eur. J. Pharmacol. 530 (1—2) (2006) 54—58.

[21] S. Ferre, V. Casado, L.A. Devi, M. Filizola, R. Jockers, M.J. Lohse, G. Milligan, J.P. Pin, X.G. Guitart, Protein-coupled receptor oligomerization revisited: functional and pharmacological perspectives, Pharmacol. Rev. 66 (2) (2014) 413—434.

[22] J.J. Rodriguez, K. Mackie, V.M. Pickel, Ultrastructural localization of the CB1 cannabinoid receptor in mu-opioid receptor patches of the rat caudate putamen nucleus, J. Neurosci. 21 (3) (2001) 823—833.

[23] M. Hojo, Y. Sudo, Y. Ando, K. Minami, M. Takada, T. Matsubara, M. Kanaide, K. Taniyama, K. Sumikawa, Y. Uezono, Mu-opioid receptor forms a functional heterodimer with cannabinoid CB1 receptor: electrophysiological and FRET assay analysis, J. Pharmacol. Sci. 108 (3) (2008) 308—319.

[24] C. Fernandez-Fernandez, L.F. Callado, R. Giron, E. Sanchez, A.M. Erdozain, J.A. Lopez-Moreno, P. Morales, de F. Rodriguez, J. Fernandez-Ruiz, P. Goya, et al., Combining rimonabant and fentanyl in a single entity: preparation and pharmacological results, Drug Des. Dev. Ther. 8 (2014) 263—277.

[25] A. Mollica, S. Pelliccia, V. Famiglini, A. Stefanucci, G. Macedonio, A. Chiavaroli, G. Orlando, L. Brunetti, C. Ferrante, S. Pieretti, et al., Exploring the first rimonabant analog-opioid peptide hybrid compound, as bivalent ligand for CB1 and opioid receptors, J. Enzym. Inhib. Med. Chem. 32 (1) (2017) 444—451.

[26] M. Le Naour, E. Akgun, A. Yekkirala, M.M. Lunzer, M.D. Powers, A.E. Kalyuzhny, P.S. Portoghese, Bivalent ligands that target mu opioid (MOP) and Cannabinoid1 (CB1) receptors are potent analgesics devoid of tolerance, J. Med. Chem. 56 (13) (2013) 5505—5513.

[27] A. Holdcroft, M. Smith, A. Jacklin, H. Hodgson, B. Smith, M. Newton, F. Evans, Pain relief with oral cannabinoids in familial mediterranean fever, Anaesthesia 52 (5) (1997) 483—486.

[28] I.D. Meng, B.H. Manning, W.J. Martin, H.L. Fields, An analgesia circuit activated by cannabinoids, Nature 395 (1998) 381—383.

[29] I. Bushlin, R. Rozenfeld, L.A. Devi, Cannabinoid-opioid interactions during neuropathic pain and analgesia, Curr. Opin. Pharmacol. 10 (1) (2010) 80—86.

[30] H. Zhang, D.M. Lund, H.A. Ciccone, W.D. Staatz, M.M. Ibrahim, T.M. Largent-Milnes, H.H. Seltzman, I. Spigelman, T.W. Vanderah, Peripherally restricted cannabinoid 1 receptor agonist as a novel analgesic in cancer-induced bone pain, Pain 159 (2018) 1814—1823.

[31] K. Monory, E. Greiner, N. Sartania, L. Sallai, Y. Pouille, H. Schmidhammer, J. Hanoune, A. Borsodi, Opioid binding profiles of new hydrazone, oxime, carbazone and semicarbazone derivatives of 14-alkoxymorphinans, Life Sci. 64 (22) (1999) 2011—2020.

[32] P.M. Beardsley, M.D. Aceto, C.D. Cook, E.R. Bowman, J.L. Newman, L.S. Harris, Discriminative stimulus, reinforcing, physical dependence, and antinociceptive effects of oxycodone in mice, rats, and rhesus monkeys, Exp. Clin. Psychopharmacol 12 (3) (2004) 163—172.

[33] M. Narita, A. Nakamura, M. Ozaki, S. Imai, K. Miyoshi, M. Suzuki, T. Suzuki, Comparative pharmacological profiles of morphine and oxycodone under a neuropathic pain-like state in mice: evidence for less sensitivity to morphine, Neuropsychopharmacology 33 (5) (2008) 1097—1112.

[34] W. Leppert, Pain management in patients with cancer: focus on opioid analgesics, Curr. Pain Headache Rep. 15 (4) (2011) 271—279.

[35] W.H. McGregor, L. Stein, J.D. Belluzzi, Potent analgesic activity of the enkephalin-like tetrapeptide H-Tyr-D-Ala-Gly-Phe-NH2, Life Sci. 23 (13) (1978) 1371—1376.

[36] D.H. Coy, A.J. Kastin, M.J. Walker, R.F. McGivern, C.A. Sandman, Increased analgesic activities of a fluorinated and a dimeric analogue of [D-Ala2]-Methionine enkephalinamide, Biochem. Biophys. Res. Commun. 83 (3) (1978) 977—983.

[37] A.W. Lipkowski, A.M. Konecka, I. Sroczynska, Double-enkephalins synthesis, activity on Guinea-pig ileum, and analgesic effect I, Peptides 3 (4) (1982) 697—700.

[38] J.L. Wiley, D.R. Compton, D. Dai, J.A. Lainton, M. Phillips, J.W. Huffman, B.R. Martin, Structure-activity relationships of indole- and pyrrole-derived cannabinoids, J. Pharmacol. Exp. Ther. 285 (3) (1998) 995—1004.

[39] M.M. Aung, G. Griffin, J.W. Huffman, M. Wu, C. Keel, B. Yang, V.M. Showalter, M.E. Abood, B.R. Martin, Influence of the N-1 alkyl chain length of cannabimimetic indoles upon CB(1) and CB(2) receptor binding, Drug Alcohol Depend. 60 (2) (2000) 133—140.

[40] J.W. Huffman, G. Zengin, M.-J. Wu, J. Lu, G. Hynd, K. Bushell, A.L.S. Thompson, S. Bushell, C. Tartal, D.P. Hurst, et al., Structure—activity relationships for 1-alkyl-3-(1-Naphthoyl)Indoles at the cannabinoid CB1 and CB2 receptors: steric and electronic effects of naphthoyl substituents. New highly selective CB2 receptor agonists, Bioorg. Med. Chem. 13 (1) (2005) 89—112.

[41] J.L. Wiley, J.A. Marusich, J.W. Huffman, Moving around the molecule: relationship between chemical structure and in vivo activity of synthetic cannabinoids, Life Sci. 97 (1) (2014) 55—63.

[42] Cs Tömböly, A. Péter, G. Tóth, In vitro quantitative study of the degradation of endomorphins, Peptides 23 (9) (2002) 1573—1580.

[43] R. Lindigkeit, A. Boehme, I. Eiserloh, M. Luebbecke, M. Wiggermann, L. Ernst, T. Beuerle, Spice: a never ending story? Forensic Sci. Int. 191 (1—3) (2009) 58—63.

[44] A. Mollica, F. Pinnen, F. Feliciani, A. Stefanucci, G. Lucente, P. Davis, F. Porreca, S.-W. Ma, J. Lai, V.J. Hruby, New potent biphalin analogues containing p-Fluoro-l-Phenylalanine at the 4,4′ positions and non-hydrazine linkers, Amino Acids 40 (5) (2011) 1503—1511.

[45] S. Nakagawa, M.A. Deli, H. Kawaguchi, T. Shimizudani, T. Shimono, Á. Kittel, K. Tanaka, M. Niwa, A new blood—brain barrier model using primary rat brain endothelial cells, pericytes and astrocytes, Neurochem. Int. 54 (3—4) (2009) 253—263.

[46] F.R. Walter, S. Veszelka, M. Pásztói, Z.A. Péterfi, A. Tóth, G. Rákhely, L. Cervenak, C.S. Ábrahám, M.A. Deli, Tesmilifene modifies brain endothelial functions and opens the blood-brain/blood-glioma barrier, J. Neurochem. 134 (6) (2015) 1040—1054.

[47] M.A. Deli, C.S. Ábrahám, Y. Kataoka, M. Niwa, Permeability studies on in vitro blood—brain barrier models: physiology, pathology, and pharmacology, Cell. Mol. Neurobiol. 25 (1) (2005) 59—127.

[48] J. Kalia, R.T. Raines, Hydrolytic stability of hydrazones and oximes, Angew. Chem. Int. Ed. 47 (39) (2008) 7523—7526.

[49] D.K. Kölmel, E.T. Kool, Oximes and hydrazones in bioconjugation: mechanism and catalysis, Chem. Rev. 117 (15) (2017) 10358—10376.

[50] J.W. Huffman, R. Mabon, M.J. Wu, J. Lu, R. Hart, D.P. Hurst, P.H. Reggio, J.L. Wiley, B.R. Martin, 3-Indolyl-1-naphthylmethanes: new cannabimimetic indoles provide evidence for aromatic stacking interactions with the CB(1) cannabinoid receptor, Bioorg. Med. Chem. 11 (4) (2003) 539—549.

[51] T.E. D'Ambra, K.G. Estep, M.R. Bell, M.A. Eissenstat, K.A. Josef, S.J. Ward, D.A. Haycock, E.R. Baizman, F.M. Casiano, N.C. Beglin, et al., Conformationally restrained analogues of pravadoline: nanomolar potent, enantioselective, (aminoalkyl)indole agonists of the cannabinoid receptor, J. Med. Chem. 35 (1) (1992) 124—135.

[52] D.R. Compton, L.H. Gold, S.J. Ward, R.L. Balster, B.R. Martin, Aminoalkylindole analogs: cannabimimetic activity of a class of compounds structurally distinct from delta 9-tetrahydrocannabinol, J. Pharmacol. Exp. Ther. 263 (3) (1992) 1118—1126.

[53] E. Stern, D.M. Lambert, Medicinal chemistry endeavors around the phytocannabinoids, Chem. Biodivers. 4 (8) (2007) 1707—1728.

[54] V.K. Vemuri, A. Makriyannis, Medicinal chemistry of cannabinoids, Clin. Pharmacol. Ther. 97 (6) (2015) 553—558.

[55] M.R. Price, Allosteric modulation of the cannabinoid CB1 receptor, Mol. Pharmacol. 68 (5) (2005) 1484—1495.

[56] T.F. Freund, I. Katona, D. Piomelli, Role of endogenous cannabinoids in synaptic signaling, Physiol. Rev. 83 (3) (2003) 1017—1066.

[57] M.D. Van Sickle, M. Duncan, P.J. Kingsley, A. Mouihate, P. Urbani, K. Mackie, N. Stella, A. Makriyannis, D. Piomelli, J.S. Davison, et al., Identification and functional characterization of brainstem cannabinoid CB2 receptors, Science 310 (5746) (2005) 329—332.

[58] F.S. den Boon, P. Chameau, Q. Schaafsma-Zhao, W. van Aken, M. Bari, S. Oddi, C.G. Kruse, M. Maccarrone, W.J. Wadman, T.R. Werkman, Excitability of prefrontal cortical pyramidal neurons is modulated by activation of intracellular type-2 cannabinoid receptors, Proc. Natl. Acad. Sci. U.S.A. 109 (9) (2012) 3534—3539.

[59] A.V. Stempel, A. Stumpf, H.-Y. Zhang, T. Özdoğan, U. Pannasch, A.-K. Theis, D.-M. Otte, A. Wojtalla, I. Rácz, A. Ponomarenko, et al., Cannabinoid type 2 receptors mediate a cell type-specific plasticity in the hippocampus, Neuron 90 (4) (2016) 795—809.

[60] Sz Dvorácskó, Cs Tömböly, R. Berkecz, A. Keresztes, Investigation of receptor binding and functional characteristics of hemopressin(1-7), Neuropeptides 58 (2016) 15—22.

[61] M. Bauer, A. Chicca, M. Tamborrini, D. Eisen, R. Lerner, B. Lutz, O. Poetz, G. Pluschke, J. Gertsch, Identification and quantification of a new family of peptide endocannabinoids (pepcans) showing negative allosteric modulation at CB 1 receptors, J. Biol. Chem. 287 (44) (2012) 36944—36967.

[62] V. Petrucci, A. Chicca, S. Glasmacher, J. Paloczi, Z. Cao, P. Pacher, J. Gertsch, Pepcan-12 (RVD-Hemopressin) is a CB2 receptor positive allosteric modulator constitutively secreted by adrenals and in liver upon tissue damage, Sci. Rep. 7 (1) (2017) 9560.

[63] A.S. Heimann, I. Gomes, C.S. Dale, R.L. Pagano, A. Gupta, L.L. de Souza, A.D. Luchessi, L.M. Castro, R. Giorgi, V. Rioli, et al., Hemopressin is an inverse agonist of CB1 cannabinoid receptors, Proc. Natl. Acad. Sci. U.S.A. 104 (51) (2007) 20588—20593.

[64] E. Guerrieri, J.R. Mallareddy, G. Tóth, H. Schmidhammer, M. Spetea, Synthesis and pharmacological evaluation of [3H]HS665, a novel, highly selective radioligand for the kappa opioid receptor, ACS Chem. Neurosci. 6 (3) (2015)

456–463.

[65] L.J. Sim, D.E. Selley, S.R. Childers, In vitro autoradiography of receptor-activated G proteins in rat brain by agonist-stimulated guanylyl 5'-[γ-[^{35}S] thiol-triphosphate binding, Proc. Natl. Acad. Sci. U.S.A. 92 (1995) 7242–7246.

[66] C. Salio, J. Fischer, M.F. Franzoni, K. Mackie, T. Kaneko, M. Conrath, CB1-Cannabinoid and μ-opioid receptor co-localization on postsynaptic target in the rat dorsal horn, Neuroreport 12 (17) (2001) 3689–3692.

[67] E.E. Codd, R.P. Shank, J.J. Schupsky, R.B. Raffa, Serotonin and norepinephrine uptake inhibiting activity of centrally acting analgesics: structural determinants and role in antinociception, J. Pharmacol. Exp. Ther. 274 (1995) 1263–1270.

[68] G. Espuña, D. Andreu, J. Barluenga, X. Pérez, A. Planas, G. Arsequell, G. Valencia, Iodination of proteins by IPy$_2$BF$_4$, a new tool in protein chemistry, Biochemistry 45 (19) (2006) 5957–5963.

[69] S.E. Bove, S.L. Calcaterra, R.M. Brooker, C.M. Huber, R.E. Guzman, P.L. Juneau, D.J. Schrier, K.S. Kilgore, Weight bearing as a measure of disease progression and efficacy of anti-inflammatory compounds in a model of monosodium iodoacetate-induced osteoarthritis, Osteoarthritis Cartilage 11 (11) (2003) 821–830.

[70] R. Combe, S. Bramwell, M.J. Field, The monosodium iodoacetate model of osteoarthritis: a model of chronic nociceptive pain in rats? Neurosci. Lett. 370 (2) (2004) 236–240.

[71] G. Kovács, Z. Petrovszki, J. Mallareddy, G. Tóth, G. Benedek, Gy Horváth, Characterization of antinociceptive potency of endomorphin-2 derivatives with unnatural amino acids in rats, Acta Physiol. Hung. 99 (3) (2012) 353–363.

[72] M.T. Smith, F.A. de la Iglesia, Co-administration of oxycodone and morphine and analgesic synergy re-examined, Br. J. Clin. Pharmacol. 59 (4) (2005) 486–487.

[73] K.K. Lemberg, V.K. Kontinen, A.O. Siiskonen, K.M. Viljakka, J.T. Yli-Kauhaluoma, E.R. Korpi, E.A. Kalso, Antinociception by spinal and systemic oxycodone: why does the route make a difference?: in vitro and in vivo studies in rats, Anesthesiology (Hagerst.) 105 (4) (2006) 801–812.

[74] J. Desroches, P. Beaulieu, Opioids and cannabinoids interactions: involvement in pain management, Curr. Drug Targets 11 (4) (2010) 462–473.

[75] A.S. Yekkirala, D.P. Roberson, B.P. Bean, C.J. Woolf, Breaking barriers to novel analgesic drug development, Nat. Rev. Drug Discov. 16 (8) (2017) 545–564.

[76] M. Nimczick, M. Decker, New approaches in the design and development of cannabinoid receptor ligands: multifunctional and bivalent compounds, ChemMedChem 10 (5) (2015) 773–786.

[77] S. Dvorácskó, A. Stefanucci, E. Novellino, A. Mollica, The design of multitarget ligands for chronic and neuropathic pain, Future Med. Chem. 7 (18) (2015) 2469–2483.

[78] G.A. Thakur, S.P. Nikas, C. Li, A. Makriyannis, Structural requirements for cannabinoid receptor probes, in: Cannabinoids, R.G. Pertwee, M.E. Abood (Eds.), Handbook of Experimental Pharmacology, Springer, Berlin, 2005, pp. 209–246.

[79] V. Chapman, The cannabinoid CB1 receptor antagonist, SR141716A, selectively facilitates nociceptive responses of dorsal horn neurones in the rat, Br. J. Pharmacol. 127 (8) (1999) 1765–1767.

[80] R.-X. Zhang, K. Ren, R. Dubner, Osteoarthritis pain mechanisms: basic studies in animal models, Osteoarthritis Cartilage 21 (9) (2013) 1308–1315.

[81] I. Farkas, G. Tuboly, Gy Benedek, Gy Horváth, The antinociceptive potency of N-arachidonoyl-dopamine (NADA) and its interaction with endomorphin-1 at the spinal level, Pharmacol. Biochem. Behav. 99 (4) (2011) 731–737.

[82] J.H. Cui, W.M. Kim, H.G. Lee, Y.O. Kim, C.M. Kim, M.H. Yoon, Antinociceptive effect of intrathecal cannabinoid receptor agonist WIN 55,212-2 in a rat bone tumor pain model, Neurosci. Lett. 493 (3) (2011) 67–71.